Fatigue Design Curves for Industrial Applications: A Review

Fatigue & Fracture of Engineering Materials & Structures

WILEY

FFEMS Fatigue & Fracture of Engineering Materials & Structures

INVITED REVIEW OPEN ACCESS

Fatigue Design Curves for Industrial Applications: A Review

Andrea Tridello[1] | Carlo Boursier Niutta[1] | Massimo Rossetto[1] | Filippo Berto[2] | Davide S. Paolino[1]

[1]Department of Mechanical and Aerospace Engineering, Politecnico di Torino, Turin, Italy | [2]Department of Chemical Engineering, Materials and Environment, Università La Sapienza, Rome, Italy

Correspondence: Andrea Tridello (andrea.tridello@polito.it)

Received: 4 April 2024 | **Revised:** 28 November 2024 | **Accepted:** 6 December 2024

Keywords: design curves | fatigue design | statistical analysis | strain–life | stress–life

ABSTRACT

In the present paper, a review on the design curves for safe–life fatigue design is provided. The methodologies available in the literature for the assessment of the strain–life and stress–life design curves have been analyzed, focusing also on the industrial practice for the design of critical components. The low-cycle fatigue (LCF), high-cycle fatigue (HCF), and very high cycle fatigue (VHCF) life ranges have been considered in the analyses. Design curves should take into account the randomness associated with the material parameter estimation and model it in a probabilistic framework. The analyses carried out in the paper have shown that methodologies based on shifting the median curve or the best-fitting curve by a fixed safety factor or a safety factor dependent on the reliability and confidence targets are among the most used. On the other hand, in several research works, more complex statistical models and methodologies, for example, based on the maximum likelihood principle or the bootstrap approach, have been proposed but are less widespread because they require a more complex implementation. The strengths and the weaknesses of the investigated methodologies have been discussed, providing also indications on future research trends.

1 | Introduction

The research on design methodologies against fatigue failures is fundamental for ensuring the safe use of structural components. Indeed, fatigue failure is the most critical failure mode for components used in structural applications, with 50%–90% of failures of components occurring due to fatigue [1–3]. Design against fatigue failure relies on material properties, dependent on the number of applied load cycles, which are estimated through experimental tests carried out according to International Standards [4–6]. It must be noted that the ASTM Standard E739 [4] has been recently withdrawn, but it has represented a reference standard for fatigue tests for many years. Fatigue tests are time consuming and expensive, and accordingly, the information obtained should be efficiently exploited to assess the required material properties. The safe–life approach commonly employed for the design involves the estimation of the stress–life or the strain–life relationship, depending on the application, in order to assess the allowable stress (or strain) the component is expected to withstand during its in-service life. However, the experimental variability of fatigue results is quite high and should be properly modeled and accounted for to ensure a safe design of components used in industrial applications.

In the literature, several methodologies have been proposed to fit experimental data and to assess the stress–life (or the strain–life) relationship [3, 7–9], even in a probabilistic framework. With these probabilistic models, the quantile associated with the stress– or strain–life curve can be estimated. Accordingly, high-reliability quantile curves can be considered to assess the allowable stress or strain to be considered for the design. However, this approach fails to account that the parameters that fit the experimental data with the considered model are not deterministic and depend on the sample, i.e., if another set of experimental tests is carried out, different parameters are estimated. The size of the confidence interval containing

Summary

- The models for the fatigue design curves for industrial applications are reviewed.
- The methods involving a shift of the median curve are the most widespread.
- The maximum likelihood principle for the parameter estimation is recommended.
- The research should also focus on the design curves in the VHCF life range.

the true parameter with a specified (generally larger than 90%) level of confidence also depends on the number of available experimental data and tends to reduce as the number of data increases. However, the number of experimental fatigue data is generally limited, with possible large intervals for the parameters. For example, in [10], 6–12 specimens are recommended to be tested for preliminary and research development tests, whereas 12–24 tests are recommended for design and reliability tests. As pointed out previously, high-reliability quantiles can be considered for the design, but the ASTM E739 recommends avoiding estimations below the 0.05th quantile. Accordingly, for design purposes, the uncertainty associated with the estimation process should be necessarily accounted for. This step is fundamental for assessing the fatigue stress–life or strain–life design curves. In industrial applications, different solutions have been proposed for the design curves, or for assessing the design point, depending on the specific applications and the indications of the International Standards [4–6, 11, 12]. One of the most widespread approaches is to shift the median or the best-fitting curve (stress–life or strain–life curve) by a conservative factor, generally corresponding to two or three times the experimental standard deviation [10]. This conservative safety factor attempts to consider the estimation uncertainty, without modeling, however, the number of available data and a target reliability level. Other widespread approaches overcome this weakness and are based on the assessment of the lower bound of a specific high-reliability quantile stress–life (or strain–life) curve. In this case, the design curve is generally denoted as the $R\alpha Cx_C$ curve, that is, the curve ensuring that, for each number of cycles to failure, there is a $(1-\alpha)\%$ failure probability (being α the reliability target) with $x_C\%$ confidence level. This curve represents the lower bound of the $(1-\alpha)$th quantile fatigue curves. Several methodologies have been proposed in the literature to assess the lower bound of high-reliability quantile strain–life or stress–life curves, estimated for example according to the "approximate Owen tolerance limit" [10, 13, 14] or with methodologies based on the maximum likelihood principle (MLP) or the likelihood ratio confidence interval (LRCI) [8, 15]. The choice of the initial model for fitting the data is also fundamental for a proper assessment of the design curves [8, 15–17], as well as taking into account the uncertainty associated with the applied load for assessing the design point [18, 19]. According to these analyses, the research on the statistical models for the fatigue design curves is currently of utmost importance and relevance for industrial applications, because a balance between ensuring a conservative safety margin even with respect to anomalous low-amplitude failures and an effective, not overconservative fatigue design is fundamental and should be based on the experimental data and appropriate statistical models.

In the present paper, a review on the models and methodologies available in the literature for the assessment of the fatigue design curves is provided. After introducing the organization of the paper, the models for the strain–life and stress–life design curves are described, considering the low-cycle fatigue (LCF), the high-cycle fatigue (HCF), and the very high cycle fatigue (VHCF) life ranges. Finally, a discussion on the available methodologies and the current trend of the research on this subject has been carried out. This review aims to analyze models currently employed in industrial applications and research models, to highlight their strengths and weaknesses and pointing out possible criticalities in this research field. This review could moreover guide the choice of the appropriate methodology, available in International Standards or in research papers, or represent a starting point for future research.

2 | Strain–Life and Stress–Life Fatigue Design Curves: General Considerations

In this section, indications on the organization of the paper and the notation used in this review are provided. The main classification of the literature models is based on the type of tests, that is, strain-controlled (Section 3) and stress-controlled (Section 4) fatigue tests. The second classification, on the other hand, is based on the investigated life region. Section 4.1 focuses on the HCF life region, whereas Section 4.2 focuses on the VHCF life region, considering also the influence of defects on the design curves. The third classification criterion is the chronological order. A section dedicated specifically to the LCF life region is not reported, since strain-controlled fatigue tests are generally carried out to investigate the LCF life range, with high applied stress inducing severe plastic deformations. However, strain–life tests can be also carried out to investigate longer fatigue life regimes. Accordingly, the reader is referred to Section 3.1 for models specifically developed for the LCF range.

In the literature, different notations have been used to indicate the same quantities. However, for the sake of clarity, we have tried to uniform as much as possible the notations used in different papers. Firstly, the upper case has been used for indicating a random variable (r.v. in the following), whereas the lower case has been used when the random variable equals a specific value, that is, the determination of the random variable. The number of cycles to failure has been indicated with n_f, with $y=\log_{10}(n_f)$. The applied stress amplitude and the maximum stress are indicated with s_a $(x=\log_{10}(s_a))$ and with s_{max}, respectively. ε refers to the applied strain, with $x_\varepsilon=\log_{10}(\varepsilon)$. Maximum likelihood has been moreover abbreviated as ML.

In the methodologies developed in the literature, the "approximate Owen tolerance limits" are largely employed. Accordingly, this method is worth to be introduced, with further details provided in the following sections. Owen [20] has carried out a systematic review on the use of tolerance limits in engineering

practice, which can be adopted also for fatigue analysis. The tolerance limits proposed by Owen [20] are computed, for the required tolerance level, at the investigated stress/strain levels, by shifting the median curve estimated from the experimental data $k_{\alpha,\gamma,n,\epsilon_d/s_{a,d},\epsilon/s_a}$ times the estimated standard deviation. The $k_{\alpha,\gamma,n,\epsilon_d/s_{a,d},\epsilon/s_a}$ factor depends on the selected reliability, α, and confidence levels, γ, on the number of experimental data, n, on the specific strain/stress level, ϵ/s_a, and on the distribution of the stress/strain data, $\epsilon_d/s_{a,d}$. Accordingly, $k_{\alpha,\gamma,n,\epsilon_d/s_{a,d},\epsilon/s_a}$ is not constant over the strain/stress amplitude values, with a hyperbolic trend with variable distance from the median curve. According to [21], the analytical computation of the design curve with this method can be rather complex and a design curve with one $k_{\alpha,\gamma,n,\epsilon_d/s_{a,d},\epsilon/s_a}$ factor averaged over the stress/strain range would be easier to derive in the industrial practice. The design curve based on a constant $k_{\alpha,\gamma,n,\epsilon_d/s_{a,d},\epsilon/s_a}$ factor is called in [21] the "approximate Owen curve," being only dependent on the reliability, confidence levels and data numerosity, and has been largely employed for strain–life and stress–life design curves, as detailed in Sections 3 and 4. Figure 1 compares an example of design curves estimated with the Owen method [20] and with the approximate Owen tolerance limit method [22].

According to Figure 1, the approximate design curve tends to deviate from the Owen tolerance limit curve at high- and low-stress values, ensuring however a good approximation while simplifying the computation.

It must be noted that Figure 1 schematically shows the stress–life design curve obtained with the approximation of the Owen approach. However, this approach can be also extended to the strain–life approach, by using similar factored coefficients, as reported in Section 3 and proven with examples and a thorough experimental validation.

3 | Strain–Life Fatigue Design Curves

This section focuses on the models for the assessment of the design strain–life fatigue curve. In general, strain-controlled experimental tests are carried out to investigate the LCF life range, with high applied stresses above the yield strength and inducing severe plastic deformations in the specimen. However, experimental data can be also collected at a higher number of cycles, in the HCF life region, with also runout data [13]. Therefore, the statistical models and the corresponding design curves should also account for the variation of the experimental slope due to the transition from fatigue damage induced by severe plastic deformations (LCF life range) and fatigue damage occurring in the elastic range (HCF). The Coffin–Manson and Morrow equation [6, 10, 13, 23–27], modeling the relationship between the total applied strain amplitude and the fatigue life, ϵ_t, and n_f, is largely employed for the analysis of strain–life data:

$$\epsilon_t = \epsilon_e + \epsilon_p = \frac{\sigma'_f}{E}(2n_f)^b + \epsilon'_f(2n_f)^c, \tag{1}$$

being ϵ_e the elastic deformation, ϵ_p the plastic deformation, σ'_f the fatigue strength coefficient, b the fatigue strength exponent, E the material Young's modulus, ϵ'_f the fatigue ductility coefficient, and c the fatigue ductility exponent. Accordingly, four unknown parameters are to be estimated from the experimental data. This equation has been largely employed in the literature, proving its effectiveness in fitting data obtained through strain-controlled tests, and is considered in several models for the fatigue design curves.

This section has been divided into subsections for the sake of clarity. In particular, the first section (Section 3.1) reports papers whose main approach is to shift the median curve by a conservative factor, with the assumption that the experimental data are normally distributed. This approach has been adopted by considering the strain–life trend described by the Coffin–Manson equation or by interpolating the experimental data with the best-fitting model. An important classification for these methods can be found in [28].

Section 3.2 describes the "generalized lifetime model" and the log-normal format for failure probability, aiming at defining a conservative safety margin in the design stage. Section 3.3, on the other hand, combines statistical methodologies with finite element (FE) analyses. Finally, Section 3.4 describes a procedure, based on the likelihood ratio confidence bound (LRCB), for the estimation of the design curves.

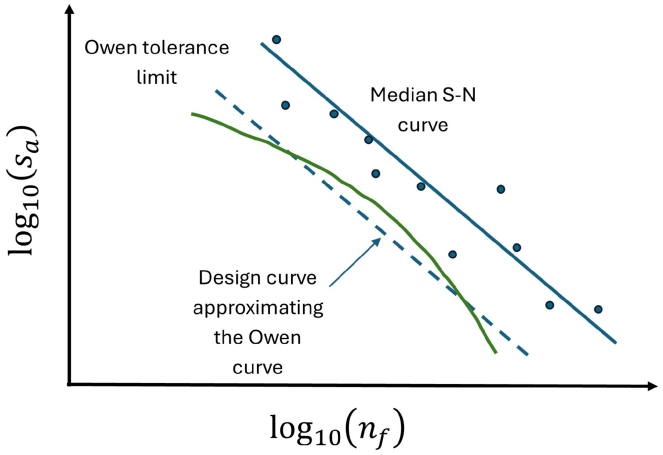

FIGURE 1 | Schematic comparison between the Owen method [20] and the approximate Owen tolerance limit method [22]. [Colour figure can be viewed at wileyonlinelibrary.com]

3.1 | Design Curve With a Conservative Shift of the Median Curve

In [28], the main approaches developed in the literature are classified into two groups, that is, the "tolerance interval" and the "equivalent prediction interval" (EPI). Even if this paper was written many years ago, that is, in 1983, approaches developed or employed later can be included within this classification.

The tolerance limit method is based on the concept of "linear failure trajectories." Each data point is crossed by a fatigue curve, the so-called failure trajectory, assumed parallel to the median curve. The failure trajectory associated with the median curve, therefore, defines the fatigue response of other experimental failures tested at different stress levels. These assumptions allow

to easily compute the design curves, with limited computational efforts. The tolerance limit at any stress level can be obtained according to Equation (2):

$$\log n_f = \hat{y} - k_{\alpha,\gamma} \cdot s, \tag{2}$$

being $k_{\alpha,\gamma}$ the tolerance factor, generally tabulated, α the reliability level, γ the confidence level, s the estimate of the standard deviation, and $\hat{y}$ the least square estimate of y_0, that is, the expected value of Y for a specific $\log\Delta\varepsilon$. $k_{\alpha,\gamma}$ has been considered constant or dependent on the reliability and confidence levels, as detailed in the following, depending on the application and the specific industrial practice.

The EPI has been proposed in Wirsching and Hseih [29]. According to this method, an equivalent constant standard deviation of Y, σ_0, can be defined according to Equation (3):

$$\sigma_0 = s \cdot g(n, \alpha), \tag{3}$$

being $g(n, \alpha) \geq 1$ a corrective factor for the standard deviation accounting for the uncertainty associated with the constant coefficients of the linear regression. Practically, a linear model is considered to fit the data, with an enlarged value of the standard deviation, so that the median curve is shifted downward.

Within the first group defined in [28] can be included methodologies that have been largely employed for specific industrial applications. For nuclear applications, the ASME code [30] suggests shifting the curve ensuring the best fit of the experimental data by a safety margin of 20 by considering the number of cycles to failure or by a factor of 2 by considering the strain amplitude. This simplified approach aims at conservatively considering/modeling the uncertainty associated with the material and loading condition. However, according to [31], this approach does not take into account environmental effects and, in particular, the influence of the light water reactor coolant, which has a significant influence on the fatigue response in this application. According to [31], the fatigue life in water with respect to the fatigue life in air can be 12 times smaller for austenitic stainless steels, 3 times smaller for Ni–Cr–Fe alloys, 17 times smaller for carbon and low-alloy steel. The influence of the reactor coolant on the fatigue life is accounted for with a corrective factor, F_{en}, defined as the ratio between the life in air at controlled room temperature and the fatigue life in water in service temperature. In [31], different formulations retrieved from the literature and based on tabulated coefficients are proposed for the computation of the factor F_{en}, dependent on the material (e.g., carbon steel and low-alloy steel). Practically, the proposed F_{en} can be integrated into the approach proposed in the ASME code.

In particular, in [31], the authors also analyze the design curves estimated according to the ASME code to show the importance of taking into account the environmental condition, whose influence depends also on several factors (like materials, strain rate, and temperature). The model reported in Equation (4) has been used for fitting the experimental data:

$$\varepsilon_a = b \cdot n_f^{-\beta} + a. \tag{4}$$

According to Equation (4), the strain–life curve ends with an asymptotic trend [31, 32], differently from the model used in [28]. The Coffin–Manson and Morrow equation has not been used in the above-analyzed papers, but a linear model or the model in Equation (4) in a bilogarithmic strain–life plot has been considered, without discriminating between the plastic and the elastic deformation contribution.

In [13], the design curves are, on the other hand, assessed by considering the Coffin–Manson and Morrow model. In particular, the strain–life curves for the plastic and the elastic range are estimated through the application of the least square method. Thereafter, the elastic and plastic strain–life design curves are obtained with the approximate Owen tolerance limit, that is, by shifting the median curve by a factor obtained by multiplying the standard deviation for the k-factors for the approximate Owen tolerance limits, reported in [13], dependent on the dataset numerosity, the confidence and the reliability levels. The plastic and elastic strain–life design curves are finally combined, according to Equation (1), to obtain the trend for the total strain amplitude with respect to the number of cycles to failure. This approach is effective, because it accounts for the dataset numerosity and the estimation uncertainty, and it has been validated on different steels [13, 33].

In [14], different approaches for the design curves are compared. The first one is called the "deterministic approach," for which the estimators of the constant coefficients are assumed as the true values and the $k_{\alpha,\gamma}$ factor in Equation (2) is assumed constant and equal to 2 or 3, that is, the median curve is shifted by two or three standard deviations. The second one is the "1d tolerance interval," with the $k_{\alpha,\gamma}$ factor in Equation (2) corresponding to the factor for a one-sided tolerance limit for a univariate normal distribution [21]. According to [21], this method can be used only when samples are tested at a unique stress level, but it has also been employed for two-dimensional regression. The third one is the method based on the approximate Owen tolerance limit, described in Section 2 and recalled in [13]. The fourth method is based on the "prediction interval," a probabilistic band including at the specific confidence level the fatigue life in future experiments. This approach accounts for the uncertainty of the estimators and the variability associated with the future predictions, justifying why the prediction bands are generally wider than the confidence band. For the design curves, the prediction interval can be computed as

$$k_{pred} = t_{1-\alpha;n-2} \cdot \sqrt{1 + \frac{1}{n} + \frac{(\varepsilon - \bar{\varepsilon})^2}{\sum_{i=1}^{n}(\varepsilon - \bar{\varepsilon})^2}}, \tag{5}$$

being $t_{1-\alpha;n-2}$ the $(1-\alpha)$th quantile from the t-Student distribution with $n-2$ degrees of freedom and $\bar{\cdot}$ indicating an average value. According to Equation (5), the design curves obtained with this method follow a hyperbolic trend, because they are dependent on ε and therefore have not been investigated in the analyses carried out by the authors. The EPI method, described at the beginning of this section, has been also recalled in [14] and considered in the comparison.

The design strain amplitudes, obtained through tests on CuAg alloy specimens for thermomechanical applications at different temperatures (room temperature, 250°C, and 300°C) and

computed with the described methods at the reversal to failure $2N_f = 2 \cdot 10^5$ cycles, have been compared. Table 1 reports the ratio between the design strain amplitude (ε_d) at 1% failure probability and with a confidence level of $\gamma = 90\,\%$ and the strain amplitude computed at $\alpha = 50\,\%$ ($\varepsilon_{50\%}$).

According to Table 1, the deterministic approach provides the least conservative design strain, with about a 12% difference with respect to the Owen method, which is, on the other hand, the most conservative approach. The difference between the *EPI*, the *1d tolerance interval* and the *approximate Owen method* is, however, limited and smaller than 3%. Accordingly, it can be concluded that these three methods provide similar results and can be equivalently employed.

3.2 | Generalized Lifetime Model and Log-Normal Format for Failure Probability

More recently, rather than focusing on the factor for shifting the median curve given a reliability or confidence level, researchers have focused their attention on the statistical distribution of the fatigue life or the strain amplitude, to subsequently derive the design curves. For example, in [34], the confidence bounds for the median curve are estimated, showing that the mean square error (MSE) should be considered preferentially for their estimation. The model used in [34] is called the "generalized lifetime model," and the lifetime cumulative distribution function (cdf) ($F(t|L)$) can be expressed with a Weibull distribution, according to the following equation:

$$F(t|L) = 1 - e^{-\left\{-\left[\beta \cdot (\Delta\varepsilon)^{\rho} \cdot t\right]^{\alpha}\right\}}, \tag{6}$$

being β, α, and ρ constant coefficients to be estimated from the experimental data and L a time-dependent load function (generally assumed constant and dependent on the strain amplitude). The confidence interval for the median curve has been also estimated, but no indications for the confidence intervals associated with a high-reliability quantile are provided.

TABLE 1 | Comparison between the methodologies for the design curve proposed in the literature and investigated in [14].

Test type	Approach	$\frac{\varepsilon_d}{\varepsilon_{50\%}}$
Room temperature	Deterministic approach	77%
	EPI	68%
	1d tolerance interval	66%
	Owen method	65%
250°C	Deterministic approach	79%
	EPI	69%
	1d tolerance interval	68%
	Owen method	66%
300°C	Deterministic approach	82%
	EPI	72%
	1d tolerance interval	72%
	Owen method	70%

The objective of the research activity in Beretta et al. [18] was to define a safety margin for components, like turbine blades, subjected to fatigue loads in the LCF life range. The authors pointed out that the safety margin and the design points cannot be defined only by considering the variability associated with the material resistance, but the scatter associated with the load in service conditions must be also accounted for. The starting model is the Coffin–Manson and Morrow relationship (Equation 1), with $\log_{10}(N_f)$ assumed to follow a normal distribution. Thereafter, the statistical distribution of ε_t and a simple format for the computation of the failure probability of parts subjected to failures in the LCF life range has been developed. In particular, with a first-order approximation (FOA) and by considering the applied stress following a normal distribution, the total strain amplitude has been assumed to follow a log-normal distribution. Similarly, the fatigue life has been shown to follow a log-normal distribution. Accordingly, the probability of failure P_f of a component has been defined in [18] as

$$P_f = Pr\left[N_f < \hat{n}_f\right] = \phi\left(\frac{\hat{n}_f - \mu_{\log(N_f)}}{\sigma_{\log(N_f)}}\right), \tag{7}$$

being Pr the notation used for "probability," ϕ the normal cdf, $\mu_{\log(N_f)}$ and $\sigma_{\log(N_f)}$ the parameters of the distribution of the fatigue life N_f.

By considering the design of a component subjected to a strain amplitude $\hat{\varepsilon}$ for a design life $\hat{n}_f$, the probability of failure has been also defined as:

$$P_f = Pr\left[\hat{\varepsilon} > \varepsilon_R\right] = \int_0^{\infty} f_{\hat{\varepsilon}}(\varepsilon) \cdot F_{\varepsilon_R}(\varepsilon) \cdot d\varepsilon, \tag{8}$$

being ε_R the strain resistance at $\hat{n}_f$. Under the FOA approximation, $\log_{10}(\varepsilon_R)$ can be approximated with a normal distribution, with parameters depending on the number of cycles to failure. Because $\log_{10}(\varepsilon_R)$ and $\log_{10}(\varepsilon)$ have been assumed normally distributed, the probability of failure becomes

$$P_f = Pr\left[\hat{\varepsilon} > \varepsilon_R\right] = \phi\left(\frac{\mu_{\log(\varepsilon_r)} - \mu_{\log(\hat{\varepsilon})}}{\sqrt{\sigma^2_{\log(\varepsilon_r)} + \sigma^2_{\log(\hat{\varepsilon})}}}\right), \tag{9}$$

being $\mu_{\log(\varepsilon_r)}$ and $\mu_{\log(\hat{\varepsilon})}$ the mean values of the distribution of $\log(\varepsilon_r)$ and $\log(\hat{\varepsilon})$, respectively, and $\sigma_{\log(\varepsilon_r)}$, $\sigma_{\log(\hat{\varepsilon})}$ the standard deviations of $\log(\varepsilon_r)$ and $\log(\hat{\varepsilon})$, respectively. The methodology and the feasibility of the FOA approximation have been successfully validated by considering two experimental databases and through Monte Carlo simulations. Finally, the log-normal distribution for failure probability has been exploited for assessing the design point ($\hat{n}_f$, $\hat{\varepsilon}$ corresponding to a target failure probability), according to Figure 2. Figure 2a plots the definition of design point, whereas Figure 2b focuses on the safety factor.

According to Figure 2a, the distance between the two mean values of $\hat{\varepsilon}$ and ε_R is equal to $\beta \cdot \sqrt{\sigma^2_{\log(\varepsilon_r)} + \sigma^2_{\log(\hat{\varepsilon})}}$, with mean ratio:

$$\frac{\mu_{\log(\epsilon_r)}}{\mu_{\log(\hat{\epsilon})}} = e^{\left[\beta \cdot \sqrt{\sigma^2_{\log(\epsilon_r)} + \sigma^2_{\log(\hat{\epsilon})}}\right]}, \tag{10}$$

with β being the safety margin. The safe–life $\hat{n}_f$ can be computed for a specific probability level and for the $\hat{\epsilon}$ value applied in service conditions, or it can be computed iteratively to obtain the desired β value. According to Figure 2b, a partial safety factor γ_F (indicated with Y_F in the figure) can be also computed, for example, by considering the 0.1% percentile ($\mu - 3 \cdot \sigma$) curve according to Equation (11):

$$\gamma_F = e^{\left[\left(\mu_{\log(\epsilon_r)} - 3 \cdot \sigma_{\log(\epsilon_r)}\right) - \mu_{\log(\hat{\epsilon})}\right]}. \tag{11}$$

An example of the proposed method is reported in Figure 3, obtained through tests on ferritic–martensitic 12%Cr steel at $T = 500°C$. In the figure, the $CV_{\hat{S}}$ value is the coefficient of variation of the applied stress, accounting for the variability associated with the applied stress and modeled with a normal distribution in [18]. The design point has been computed for a safety margin $\beta = 3.8$, corresponding to a probability of failure of $7 \cdot 10^{-5}$, characteristic of "safety critical components." The authors concluded that, for different steels, the typical safety factors are in the range [1.15–1.6], pointing out that in the plastic regime, the safety factor should be increased, due to the higher experimental scatter.

3.3 | Statistical Modeling and FE Analyses

In [19], the procedure developed in [18] has been extended, focusing on the multiaxial LCF design, which typically occurs in

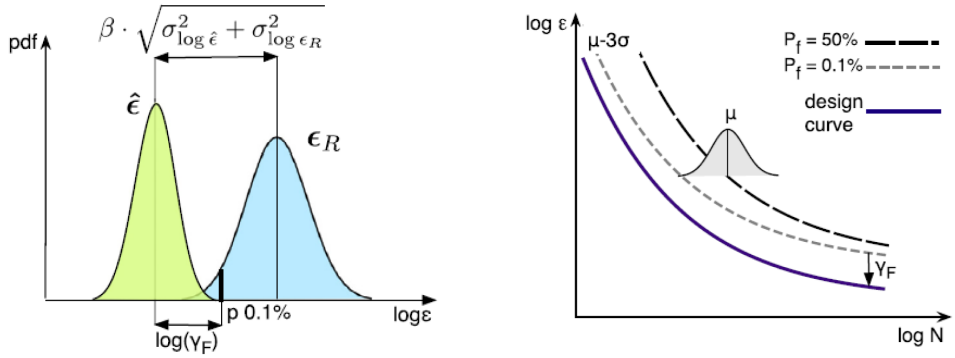

FIGURE 2 | Design methodology in [18] at a target reliability level: (a) definition of design point (being γ_F the safety factor, according to Equation 11) and (b) design curve by exploiting the safety factor concept. Reprinted with permission from Elsevier. [Colour figure can be viewed at wileyonlinelibrary.com]

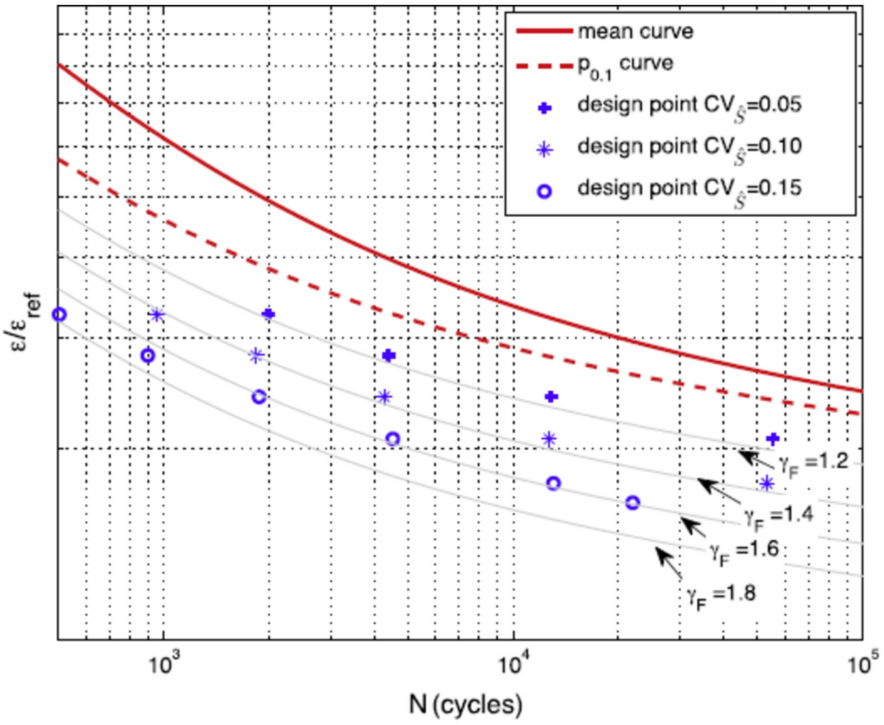

FIGURE 3 | Experimental validation of the procedure proposed in [18]. Reprinted with permission from Elsevier. [Colour figure can be viewed at wileyonlinelibrary.com]

notched parts. In particular, the authors pointed out that the elastic–plastic behavior of components is generally modeled and simulated by considering deterministic material parameters obtained with controlled experimental tests. Accordingly, the procedure in [19], based on commercial numerical and simulation software, like Matlab and Ansys, accounts for the material variability as input and is based on a probabilistic FOA model [18]. The developed procedure is summarized in Figure 4 and has been validated on notched specimens.

According to Figure 4, a structural model of the notched component is created, together with the distribution of the material parameters and the variability associated with the load, computed according to load spectrum analysis. Thereafter, an iterative process is set, with the random generation of 10^3 populations of material parameters and loads. For the ith iteration, the cyclic response and the corresponding scatter are assessed, with a subsequent curve fitting with the Chaboche and Fatemi–Socie model. The objective of this step is the parameter identification. Then, a nonlinear FE model of the notched component is defined to assess the element with the maximum Fatemi–Socie equivalent shear strain amplitude and the critical plane with the Fatemi–Socie criterion. The corresponding number of cycles to failure is assessed with the Manson–Coffin and Morrow equation modified by considering the Fatemi–Socie criterion and the equivalent shear strain amplitude. A second iterative process based on the 10^3 samples to

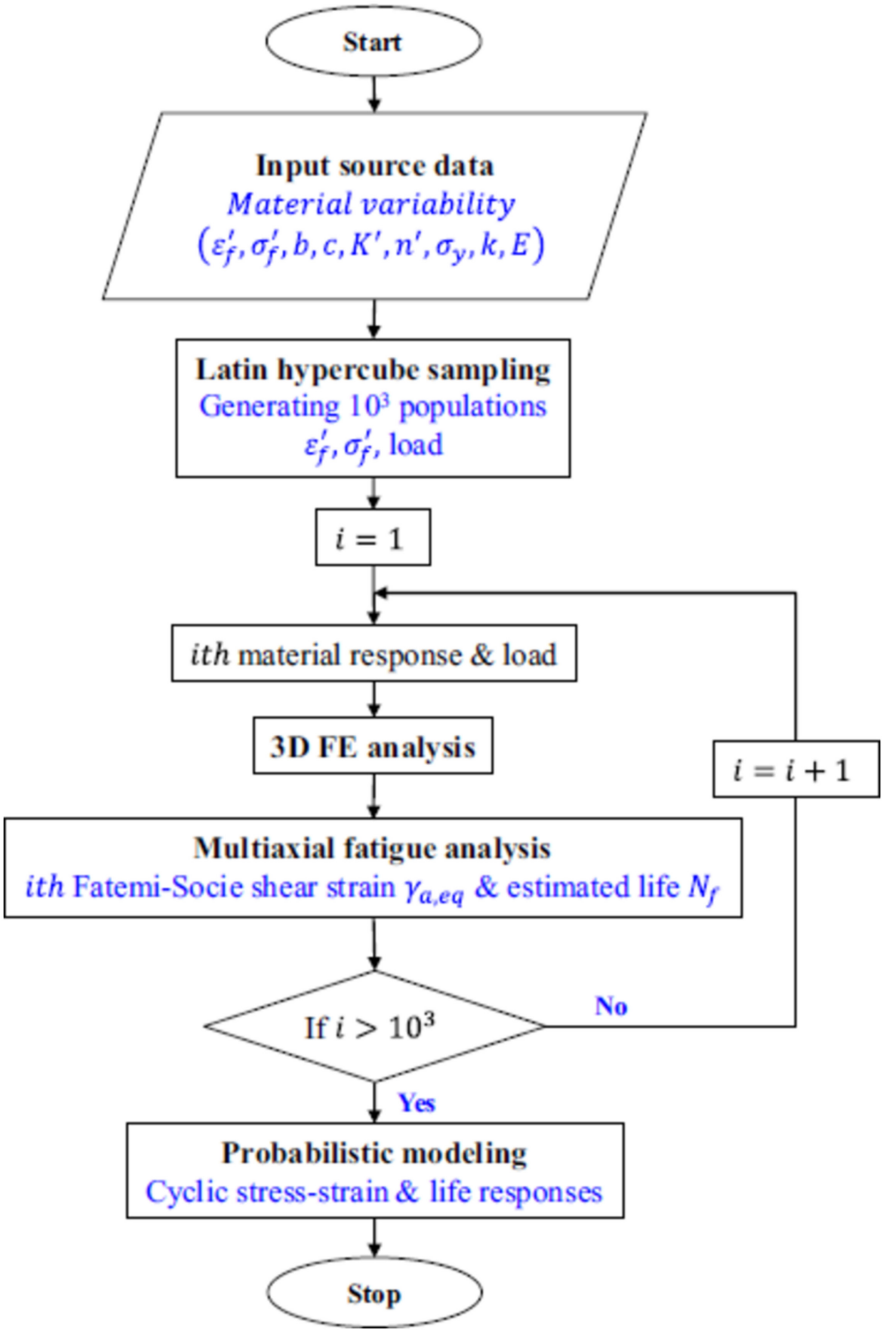

FIGURE 4 | Flow chart of the procedure developed in [19] for the analysis of the LCF response under multiaxial loads. Reprinted with permission from Elsevier. [Colour figure can be viewed at wileyonlinelibrary.com]

assess the influence of the material and load variability on the cyclic stress–strain and strain–life behavior of the investigated component is set. The cyclic stress–strain response, the life scatter, and the safety factors under multiaxial LCF design are obtained at the end of this procedure, with the probability of failure, computed with FOA, and the design point at the selected reliability finally assessed. With the FOA, the probability of failure can be computed according to Equation (9) (defined in [18]), by considering the equivalent shear strain amplitude $\gamma_{a,eq}$ in place of the strain amplitude. For details on the implementation procedure, the reader is referred to [19].

Figure 5 plots the equivalent shear strain amplitude, $\gamma_{a,eq}$, with respect to the number of cycles to failures for data points obtained by considering the properties of a 9CrMo steel at a temperature of 550°C, with increasing safety factors γ_f, for a $CV_S = 0.1$ and a safety margin β equal to 3.8 for the design point. According to Figure 5, the safety factor is between 1.9 and 2.5, with simulated failures at a safety distance from the design points.

3.4 | LRCB for the Design Curve

Finally, in [35], the statistical distribution of the total strain amplitude and the fatigue life is analytically obtained, starting from the Manson–Coffin and Morrow model, and the design curves are obtained as the LRCB of a high-reliability quantile. A log-normal distribution has been assumed for the total strain and for the elastic strain, showing that the plastic strain can be considered also approximately log-normal. The cdf of the elastic strain, $F_{E_e}(\varepsilon_e;\mu_e,\sigma_e)$, has been defined as

$$\begin{cases} F_{E_e}(\varepsilon_e;\mu_e,\sigma_e) = \phi_G\left(\dfrac{\ln(\varepsilon_e)-\mu_e}{\sigma_e}\right), \\ \mu_e = \ln\left(\dfrac{\sigma_f'}{E}\right) + b\ln(2n_f) = a_e + b_e\ln(n_f) = a_e + b_e y, \end{cases} \tag{12}$$

being $\phi_G(\cdot)$ the standardized normal cdf and a_e and b_e constant coefficients to be estimated from the experimental data. Similarly, the cdf of the plastic strain, $F_{E_p}(\varepsilon_p;\mu_p,\sigma_p)$, has been defined as

$$\begin{cases} F_{E_p}(\varepsilon_p;\mu_p,\sigma_p) = \phi_G\left(\dfrac{\ln(\varepsilon_p)-\mu_p}{\sigma_p}\right), \\ \mu_p = \ln\left(\varepsilon_f'\right) + c\ln(2n_f) = a_p + b_p\ln(n_f) = a_p + b_p y, \end{cases} \tag{13}$$

being a_p and b_p constant coefficients to be estimated from the experimental data. From Equations (12) and (13), and with the passages defined in [35], the cdf of the fatigue life, $F_{n_f|E_t}(\varepsilon_t;\mu_t(n_f),\sigma_t(n_f))$ for a given total deformation, ε_t, is obtained:

$$F_{n_f|E_t}(\varepsilon_t;\mu_t(n_f),\sigma_t(n_f)) = F_{N_f|\varepsilon_t}(n_f;\varepsilon_t) = \phi_G\left(\frac{\ln(\varepsilon_t)-\mu_t(n_f)}{\sigma_t(n_f)}\right), \tag{14}$$

being $\mu_t(n_f)$ and $\sigma_t(n_f)$ the mean and the standard deviation of the cdf of the fatigue life. According to [35], μ_t and σ_t depend on the constant parameters in the Manson–Coffin and Morrow model (Equations 12 and 13). The probability density function (pdf, $f_{n_f|E_t}(\varepsilon_t;\mu_t(n_f),\sigma_t(n_f))$) of the fatigue life has been also obtained analytically. Accordingly, given the cdf and the pdf of the distribution, the parameter estimation can be computed by applying the MLP, to consider both failure and runout data, which are neglected with other methodologies based on the least square method [13]. The procedure for parameter estimation is summarized in Figure 6. In the figure, the notation $\tilde{}$ indicates an estimate of the specific parameter, $L[\boldsymbol{\theta}]$ is the Likelihood function, with $\boldsymbol{\theta}$ the vector of the parameters to be estimated, n is the number of failures, n_r is the number of runout data, i_f and j are the counter for the number of failures and runout data, and n_f^* is the runout number of cycles.

According to Figure 6, the slope and the intercept for the elastic (a_e and b_e) and plastic (a_p and b_p) ranges are estimated through a linear regression by considering the trend of the elastic and plastic data, respectively, with respect to the fatigue life. $\rho_{e,p}$

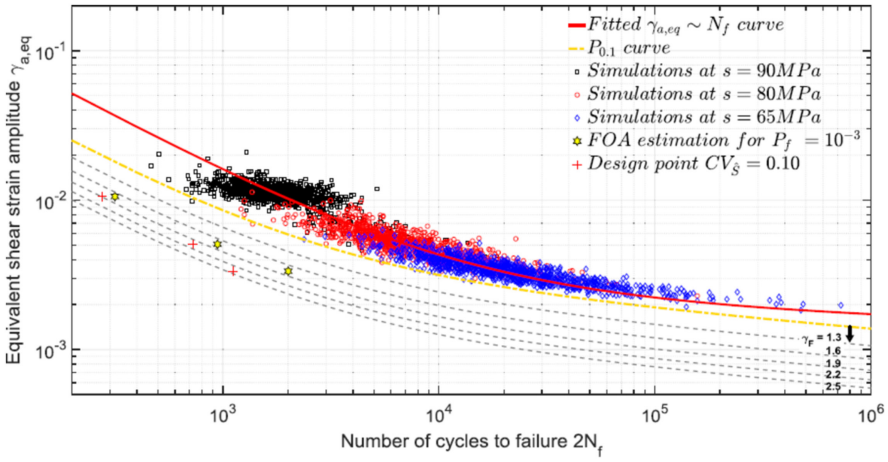

FIGURE 5 | Equivalent shear strain amplitude with respect to the number of cycles to failure in [19] to validate the developed procedure. Reprinted with permission from Elsevier. [Colour figure can be viewed at wileyonlinelibrary.com]

is the correlation coefficient between the experimental elastic and plastic strain amplitudes. Given the coefficients describing the linear trend in the elastic and in the plastic range and the correlation coefficients, the standard deviations for these two ranges are the only unknown values. They are estimated by applying the MLP, that is, by maximizing the Likelihood Function, $L[\boldsymbol{\theta}]$. In particular, the unknown standard deviation parameters contained in the $\boldsymbol{\theta}$ vector are iteratively varied within an optimization process in order to maximize the likelihood function.

Finally, the design curves are estimated as the LRCB of a high-reliability quantile strain–life curve. In particular, for each n_f in the range of interest, the lower bound of the selected quantile at the $\alpha\%$ reliability level, $\varepsilon_{t,\alpha}$, is obtained by solving Equation (15):

$$PL\left[\varepsilon_{t,\alpha}\right] = \frac{\max_{\theta_2}\left[L\left[\varepsilon_{t,\alpha},\theta_2\right]\right]}{L\left[\widetilde{\boldsymbol{\theta}}\right]} \geq e^{-\frac{\chi^2(1;1-\beta_{th})}{2}}, \tag{15}$$

where $PL\left[\varepsilon_{t,\alpha}\right]$ is the profile likelihood function, $L\left[\widetilde{\boldsymbol{\theta}}\right]$ is the likelihood function computed for the set of parameters $\widetilde{\boldsymbol{\theta}}$ estimated according to the procedure in Figure 6, and $\chi^2\left(1;1-\beta_{th}\right)$ is the $\left(1-\beta_{th}\right)$th quantile of a chi-square distribution with 1 degree of freedom. This procedure involves multiple optimizations and an iterative procedure that has been detailed in [35].

The approach in [35] has been validated by considering literature data obtained by testing different steels. In particular, Figure 7 compares the design curves estimated with the method proposed in [13], based on the *approximate Owen tolerance limit* and described previously, and the method in [35]. Figure 7 plots the data for a SAE 1137 steel and for an SAE D4512 steel. In the figures, R50 and R90 refer to the 0.5th and 0.1th percentile strain–life curves, ML refers to "maximum likelihood," [9] corresponds to [13] in the present paper, and LRCB refers to the design curve estimated with the method proposed in [35].

According to Figure 7, the two methodologies provide similar results, with the design curves characterized by very similar trends. The procedure defined in [35] can be used as an alternative to those already available in the literature and can also consider runout data, which are neglected with the other methodologies.

To conclude, in the literature, there are many available approaches for the strain–life design curves, developed for specific industrial applications. The most widespread method is the one based on shifting the median curve by a safety factor that multiplies the standard deviation and depends on the reliability, confidence levels, and dataset numerosity. This factor is generally tabulated and can be easily obtained. The model for the strain–life trend can be a simple linear model allowing the best fit of the experimental data [28] or the Manson–Coffin and Morrow model [13, 14]. More recently, the research has focused on the statistical distribution of the fatigue life to define the design points, the safety factors, and the design curves. These models can be more accurate, since, for example, can take into account the randomness associated with the applied strain or the material strength, or can consider runout data, but require a more complex implementation.

4 | Stress–Life Fatigue Design Curves: HCF and VHCF Life Ranges

This section focuses on the models for the design curves in longer life ranges, that is, in the HCF and the VHCF life regions, mainly investigated through stress-controlled tests because the applied stress is significantly below the material yield stress. Section 4.1 is about the design curves in the HCF life range, whereas Section 4.2 focuses on the design curves

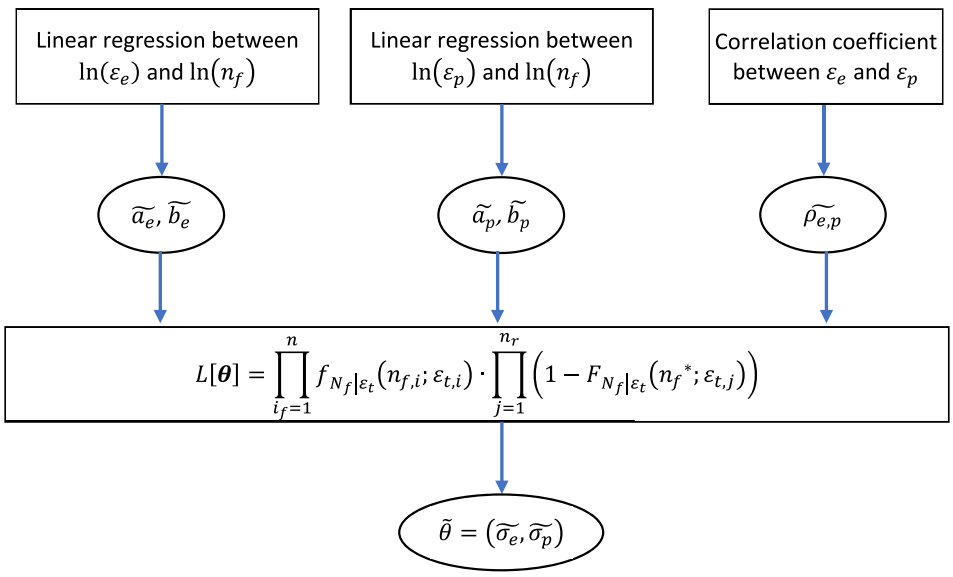

FIGURE 6 | Procedure for parameter estimation defined in [35] and based on the maximum likelihood principle. [Colour figure can be viewed at wileyonlinelibrary.com]

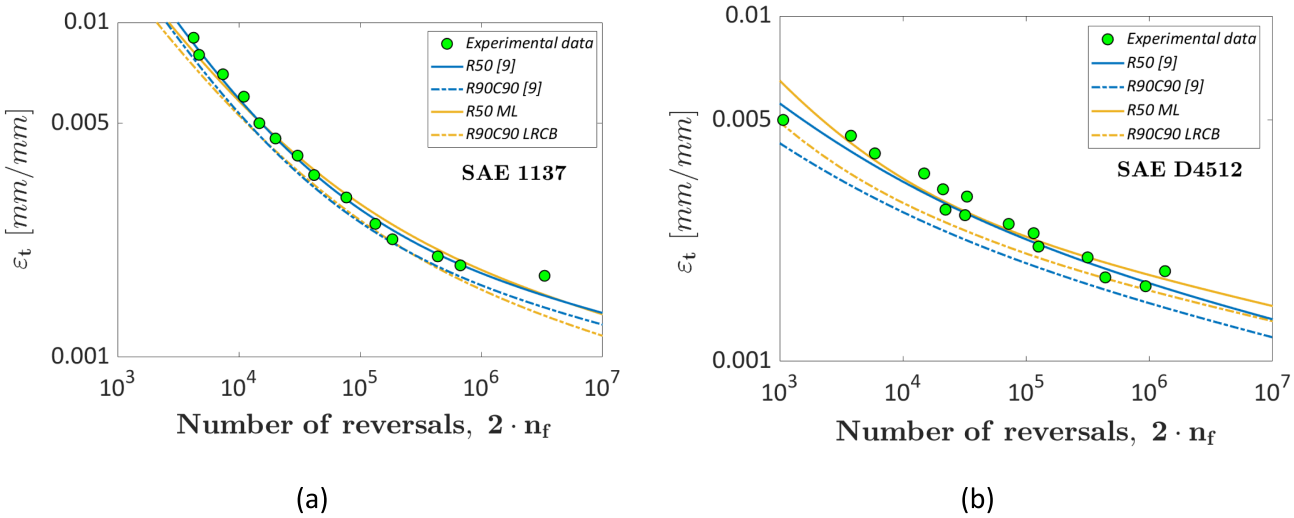

FIGURE 7 | Comparison between the design curve estimated in [35] (yellow curves) and in [13] (blue curves): (a) SAE 1137 steel and (b) SAE D4512 steel. [Colour figure can be viewed at wileyonlinelibrary.com]

in the VHCF life ranges and with failures originating from defects.

4.1 | Stress-Controlled Fatigue Tests: HCF Life Ranges

In this section, the design curves for data collected in the HCF life range, that is, above 10^3–10^4 cycles and below 10^7 cycles, with stress-controlled fatigue tests are reviewed. In this life regime, the probabilistic-*S*–*N* (P-*S*–*N*) curves generally show a linearly decreasing trend, described with a power law function (i.e., the widely known Basquin model). However, depending on the material, they may show an asymptotic trend above 10^6 cycles, the so-called fatigue limit. This behavior should be properly modeled with a high degree of reliability and confidence level, especially for design purposes. Indeed, the assumption of an asymptotic trend should be confirmed by the experimental data to prevent a nonconservative design, depending on the applications and the number of cycles the component is expected to withstand. Indeed, the concept of fatigue limit has been put under question by experimental results investigating the VHCF life range [36–38], with the conventional asymptote corresponding to the fatigue limit being considered as a transition stress between surface failures, typical of the HCF life range, and internal failures, typical of the VHCF life range. However, if the component in service condition is not expected to have a fatigue life in the VHCF life range and is not subjected to low-amplitude stress, for example, induced by high-frequency vibrations, a model with a monotonically decreasing trend and a fatigue limit can be considered and is largely employed in industrial application for the design of steel components. For materials like cast aluminum alloys, which do not show an asymptotic trend but a change of the slope of the linear trend, the FKM guideline provides indications on the slopes, equal to 5 before the knee point at 10^6 cycles and to 15 above the knee point. These trends and slopes have to be however verified and depend on the manufacturing processes, as demonstrated in [39].

This section has been divided into subsections, with the main approaches available in the literature grouped and classified for better clarity. Two main groups have been identified. Within the first group (Section 4.1.1), the approach based on a separate estimation of the linear decreasing trend in the finite life range and of the HCF limit has been analyzed. The design curve is finally estimated by shifting the median curves by a factor obtained as the product of a tabulated factor, dependent on the dataset numerosity, and the standard deviations. The second group (Section 4.1.2) includes the approaches ensuring the continuity between the finite life range and the HCF life ranges. The design curves are thereafter estimated with different methodologies, like the LRCB or the bootstrap approach. It must be noted that this subdivision is not strict, for example, the approach developed in [40] has been included within the second group, but it could be considered appropriate also for the first group. However, in authors' opinion, this is a clearer classification.

4.1.1 | Finite Life Linear Trend and HCF Limit: Shift of the Median Curve

For experimental data showing a linearly decreasing trend ending with an asymptote, the most used approach is the one reported in [10]. In particular, the fatigue limit is estimated with the staircase approach [10, 41], a popular methodology aimed at assessing the fatigue strength at a number of cycles to failure corresponding to the runout number of cycles. An asymptotic trend is generally assumed at a stress amplitude equal to the fatigue strength estimated with the staircase. Very briefly, with a staircase, the test campaign is started after a careful selection of the step *d*, which has to be as close as possible to the fatigue limit standard deviation, and the runout number of cycles. After the first test, the applied stress amplitude is increased or decreased by a stress amplitude step corresponding to the step *d*. If the test has ended with a runout, the subsequent test is carried out by increasing the applied stress amplitude by the step *d*. If the test has ended with a failure, the subsequent test is carried out by decreasing the applied stress amplitude

by step d. This procedure is repeated until an appropriate number of tests has been obtained, generally corresponding to 15 tests [3, 41]. The median fatigue limit and the standard deviation are obtained according to the formulation reported in [10] and based on the least frequent event (failure or runout). For a proper application of the method, the number of failures and runout data should be similar. These formulations have been originally developed for different applications in [42, 43] by applying the ML principle. Due to its straightforward and simple procedure, the staircase method is largely employed in industrial applications, even if it involves a nonnegligible testing effort and can be time consuming, especially if the testing frequency is low, and because tests should be carried out sequentially. According to [10], the lower bound of the fatigue limit, $s_{l,R\alpha Cx_C}$, is computed with the one-side lower bound tolerance limit k factor for a normal distribution [44]:

$$s_{l,R\alpha Cx_C} = \mu_{x_l} - k \cdot \sigma_{x_l}, \tag{16}$$

being μ_{x_l} the median value of the fatigue limit and σ_{x_l} the corresponding standard deviation. The k value is assessed by considering the required reliability and confidence levels and the numerosity of the least frequent event.

In the BS ISO [5] International Standard, a "modified staircase approach" is proposed, with a reduced number of valid specimens to be tested, provided that the standard deviation of the fatigue limit is known. The sequential approach considered for the staircase is the same and a minimum of six specimens is required. The lower value of the fatigue limit can be obtained by considering Equation (16) and the tables reported in the BS ISO [5] International Standard. However, the standard deviation of the fatigue limit is generally not known before the experimental tests and can be hardly reliably guessed from available literature data. Therefore, this approach should be employed with caution.

For the finite life range, modeled with a linearly decreasing trend in the log–log S–N plot, the most used approach to assess the lower bound design curve and suggested in [10] is based on the concept *linear failure trajectories* described in Section 3. According to [10], the constant coefficients describing the linear trend are estimated through the application of the least square method. The lower bound design curve is obtained with Equation (17):

$$\log_{10}(n_f) = \mu_Y(s_a) - k_Y \cdot \sigma_Y, \tag{17}$$

being $\mu_Y(s_a)$ and σ_Y the median value and the standard deviation of the number of cycles to failure, respectively, at a specific applied stress amplitude and k_Y a multiplicative safety factor. In industrial applications, k_Y is generally chosen equal to 2 or 3, that is, the stress–life median curve is shifted by a factor equal to two or three times the standard deviation. This approach, despite its simplicity, does not account for the required reliability, confidence level, and dataset numerosity. Accordingly, to model the uncertainty associated with the parameter estimation with the least square method, the method reported in the ASTM1998 Standard [4] and the approximate Owen one-side tolerance limit method are largely employed. The ASTM1998 Standard [4], however, provides indications only on how to estimate the double-side confidence interval for the median curve, but this may not ensure the required reliability level for the design of components. The approximate Owen one-side tolerance limit approach, on the other hand, provides the lower bound at the required confidence level, for each quantile curve, as already discussed in Section 3. The k_Y value for shifting the median curve at the required reliability and confidence levels can be obtained from the formulations reported in [33] or through tabulated values [10]. The transition point between the finite life range and the infinite life range is obtained as the intersection between the finite life curve and the fatigue limit horizontal line.

This method, which requires a separate estimation of the lower bound of the fatigue limit and of the linearly decreasing trend, is easy and straightforward, justifying its wide diffusion in the industrial practice [10]. On the other hand, the separate estimation may not ensure the continuity of the curve, especially if significantly different scatters are observed in the finite and the infinite life ranges. Moreover, the sharp transition between these two trends is not physical, with the experimental data characterized by a smoother trend when approaching the fatigue limit. Another concern with the application of this approach is that the data considered for the staircase (and the runout data) are generally not considered for the estimation of the design curve in the finite life range, even if they contain important information. Moreover, with the staircase approach, a large number of runout data has to be obtained (e.g., with 15 valid tests, seven or eight runout data are expected), significantly increasing the testing time, as discussed in [8].

Figure 8 shows an example of S–N curves estimated with an approach combining the Owen one-side tolerance limit and the staircase approach. The median and the R90C90 design curve are plotted.

4.1.2 | Models Ensuring the Continuity Between the Finite Life and the HCF Limit

According to the above-described possible criticalities associated with the application of the Owen one-side tolerance limit and the staircase method, models ensuring the continuity between the finite and the infinite life ranges have been proposed and employed. For example, in [40], the design curves estimated starting from Equation (18) have been investigated:

$$(s_a - s_0) \cdot n_f^b = c, \tag{18}$$

being s_0, b, and c constant coefficients to be estimated from the experimental data. In this work, the approach already described in Section 2 and suggested in ASME Boiler and Pressure Vessel, which requires to reduce the best-fitting curve by a factor of 20, by considering the number of cycles to failure, and of 2 or 2.5, by considering the applied stress amplitude, has been followed to estimate the design curve. These methods have been compared by analyzing the results of tests on 1Cr18Ni9Ti pipe-welded joint. The Authors concluded that a 20 factor on the number of cycles to failure and of 2.5 for the stress amplitude are both appropriate for the HCF life range, even if they are too conservative at high number of cycles. This has been justified by considering that the standard deviation is not constant with n_f and a constant factor safety factor cannot account for this experimental evidence,

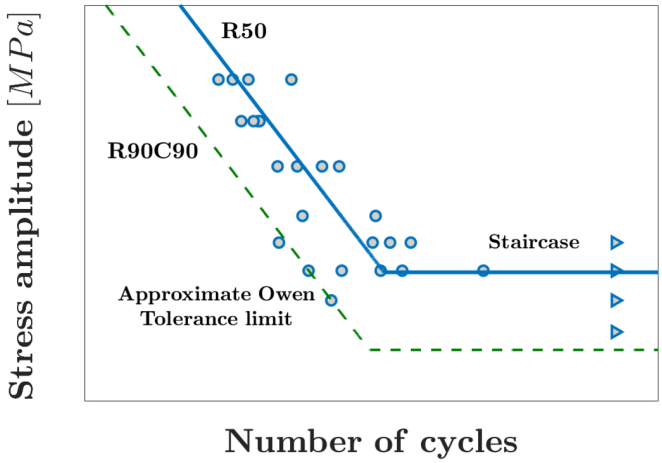

FIGURE 8 | Example of median and R90C90 design curves estimated with a method based on combining the Owen one-side tolerance limit and the staircase approach. [Colour figure can be viewed at wileyonlinelibrary.com]

with the authors suggesting the use of probabilistic and data-based approaches.

In [15], the design curves are estimated starting from the so-called "random fatigue limit model." The marginal cdf, $F_W(w;x,\theta)$, of the $W = \log_{10}(N_f)$ random variable is reported in Equation (19):

$$F_W(w;x,\theta) = \int_{-\infty}^{x} \frac{1}{\sigma_\gamma} \Phi_{W|V}\left(\frac{w-\mu(x,v)}{\sigma}\right) \cdot \phi_V\left(\frac{v-\mu_\gamma}{\sigma_\gamma}\right) \cdot dv, \quad (19)$$

being $x = \log_{10}(s_a)$; γ the fatigue limit; $v = \log_{10}(\gamma)$; $\mu(x,v)$ and μ_γ the location parameters of the fatigue life and the fatigue limit, respectively; σ and σ_γ the scale parameters of the fatigue life and the fatigue limit, respectively; and $\boldsymbol{\theta}$ the set of material parameters to be estimated from experimental data. $\Phi_{W|V}$ is the cdf of the fatigue life, given the applied stress, whereas ϕ_V is the pdf of the fatigue limit. The mean value of the fatigue life is given in Equation (20):

$$\mu(x,v) = \beta_0 + \beta_1 \cdot \log_{10}(s-\gamma). \quad (20)$$

The "random fatigue limit model" is therefore obtained by marginalizing the conditional cdf of the fatigue life, dependent on the fatigue limit γ, with respect to the pdf of the fatigue limit.

The MLP is employed in [15] for the estimation of the unknown parameters. The design curves are estimated as the LRCB of a high-reliability quantile and exploiting the properties of the profile likelihood function, according to the formulation reported in Equation (15). This choice is justified by the authors by considering that the coverage probabilities of LRCB better approximate the nominal confidence levels. The model has been validated by considering literature data. The authors compare the fitting capability of the model considering a normal distribution or the smallest extreme value (SEV) distribution for the fatigue life and a normal distribution or SEV distribution for the fatigue limit. The normal distribution for the fatigue life and the fatigue limit is the one providing the best-fitting capability. The 95% lower confidence bound for the 0.05th and the 0.01th quantile of the P-*S*–*N* curves of composite laminate data have also been estimated by considering different combinations of the statistical distributions of the fatigue life and the fatigue limit. The SEV–SEV model is for both quantiles the most conservative, providing the lowest curve. This approach and the subsequent estimation of the design curves with the LRCB have proven effective for the estimation of the design curves, being capable of modeling the experimental trend and a smooth transition between the finite and the infinite life. Moreover, the design curves are obtained in a statistical framework and not by considering a fixed shifting factor, with the possibility of selecting the statistical distribution of the fatigue life that best fits the data, rather than only the normal distribution considered for the methodologies investigated above.

In [16], the author concentrates on the fatigue limit estimation. Two models have been analyzed, with the estimation carried out with the MLP. In the first model (Model 1), the cdf of the fatigue life is given by the product of the cdf of the conditional fatigue life (conditioned to the applied stress amplitude) and of the cdf of the fatigue limit. The fatigue life and the fatigue limit are assumed normally distributed, with the mean of the finite fatigue life linearly dependent on the logarithm of the applied stress amplitude. The standard deviation of the fatigue life, on the other hand, has not been considered constant and is assumed to increase with the fatigue life, according to the experimental evidence. With this model, the fatigue limit is estimated by considering the information on the number of cycles to failure associated with each failed specimen and the runout data. The second model (Model 2), on the other hand, exploits only the information on the specimen state, that is, if it has failed or if it is a runout specimen. Literature staircase data have been used to compare the two models. Interestingly from a design point of view, the author proposes a methodology to estimate the lower bound of the fatigue limit, corresponding to the lower bound of high-reliability quantile fatigue limit, s_{e_p}, according to Equation (21):

$$\ln s_{e_p} = \hat{\mu}_{xe} - \lambda_p \cdot \hat{\sigma}_{xe} - \lambda_\alpha \cdot \sqrt{\widehat{Var}\left(\hat{\mu}_{xe} - \lambda_p \cdot \hat{\sigma}_{xe}\right)}, \quad (21)$$

being $\hat{\mu}_{xe}$ the mean of the fatigue limit distribution, λ_p and λ_α two percentiles, p the percentile, α the confidence level, $\hat{\sigma}_{xe}$ the variance of the fatigue limit distribution, Var the variance, and $\hat{\cdot}$ indicating an estimate of the considered parameter. The notation in Equation (21) is for Model 1. However, for Model 2, according to the notation used in the paper, s_{e_p} is replaced by $s_{e_{lp}}$, μ_{xe}, and σ_{xe} are replaced by μ_{xel} and σ_{xel}. With analyses on simulated and literature data, the author concluded that the information on the finite lives contained in Model 1 is effectively exploited and is positive for the estimation, even if the estimation process is more complex. The analyses have also shown that, if the two models provide fatigue limit values characterized by significant differences, the runout number of cycles should be increased. Moreover, the estimated lower confidence bounds are proven to be too high, according to the analyses on simulated datasets. However, the proposed approach represents an alternative to the

widely adopted staircase methodology, even if its implementation is more complex.

Differently from the above-analyzed method, in [45], a Bayesian approach is employed for the analysis of the fatigue data and the estimation of the design curves. The Basquin model is considered as the starting model for fitting the experimental data. This approach allows to exploit prior technological knowledge on the fatigue model parameters and their relationship with other material properties, for example, the quasistatic properties, like the ultimate tensile strength. According to the authors, this is particularly useful when the number of experimental data is limited. The proposed methodology has been validated on simulated data, which have shown that an informative prior on the variance of the logarithm of the fatigue life significantly enhances the performance of the estimation. For instance, the Bayesian R95C90 curve estimated by considering six simulated specimens provides the same design curve obtained with 12 or 24 specimens with the classical approaches, with a consequent possible reduction of the testing time. This interesting approach can represent a valid alternative to methodologies based on classical inference, provided that valid relationships between material parameters and prior knowledge on the material variability are available.

An alternative interesting approach to those described above is represented by the bootstrap approach employed in [17], validated by testing a 75S-T6 aluminum alloy. In the first part of the paper, the models for the mean fatigue life reported in Equation (18), with constant (Model Ia) and nonconstant standard deviation (Model Ib) and log-normal distribution for the fatigue lives, are considered. The random fatigue limit model with normal distribution and constant (Model IIa) and nonconstant (Model IIc) standard deviation, with SEV distribution and constant (Model IIb) and nonconstant (Model IId) standard deviations are also considered and compared. Interestingly, the confidence bands and intervals are estimated with a stratified bootstrap. In particular, the dataset is stratified on the cycle ratio, and from each stratum, 200 datasets are randomly generated. For each dataset, the ML estimate and the corresponding quantile are estimated. Figure 9 shows the estimated 95% confidence bounds for the 0.05th quantile of the fatigue life.

According to Figure 9, reasonable estimates of the confidence bound are obtained with this approach, even if failures are found below the lower bound curves, apart from Models Ia and Ib. This means that higher reliability and confidence levels are to be selected with the proposed approach. Moreover, Model Ib has an irregular and stepped trend, which is quite unusual for design P-*S*–*N* curves. However, an optimized bootstrap approach can be used and does not require assumptions on the statistical distribution of the confidence interval associated with the investigated quantile.

In [8], three models for the design curves of datasets showing a linearly decreasing trend and ending with a fatigue limit are compared. The first model is based on the staircase approach for the fatigue limit and the approximate Owen one-sided tolerance limit previously described and employed in [10]. In the second model, the cdf, $F_{Y|x}$, of the logarithm of the fatigue life, Y, conditioned to the logarithm of the applied stress amplitude, x, is given in Equation (22):

$$F_{Y|x} = \Phi\left(\frac{y-(a+b\cdot x)}{\sigma_Y}\right)\Phi\left(\frac{x-\mu_{X_l}}{\sigma_{X_l}}\right), \tag{22}$$

being $\Phi(\cdot)$ the cdf of a standardized normal distribution, μ_{X_l} and σ_{X_l} the mean and the standard deviation of the fatigue limit, a and b two constant coefficients to be estimated from the experimental data, and σ_Y the standard deviation of the fatigue life. The cdf of the fatigue life is therefore given by the product of the cdf of the finite fatigue life and the cdf of the fatigue limit, both assumed as normal. The parameter estimation is carried out by applying the MLP and the LRCB for a high-reliability quantile curve is considered the design curve, according to Equation (15). Finally, the bootstrap approach is exploited for estimating the design curves. Starting from the model in Equation (22) and once the parameter estimation has been carried out with the MLP, n_S datasets replicating the initial dataset are randomly generated. Thereafter, the parameter estimation is carried out for each simulated dataset and the P-*S*–*N* curves at the quantile of interest are estimated. This procedure is iteratively repeated for at least 1000 datasets. Finally, for each n_f, the simulated stress amplitudes at the quantile of interest are sorted in ascending order and the stress amplitude at the $n_S \cdot (1 - x_C/100)$ position is the lower bound design stress amplitude at the x_C confidence level.

These three methodologies have been compared by considering the experimental results obtained by testing materials used in the automotive sectors, that is, a *TRIP-assisted bainitic steel TBC600Y980T*, an *aluminum alloy G-AS7C3,5GM*, and a composite material *Polynt SMC LP 2512 R33*. Figure 10 compares the R90C90 design curves estimated with the investigated methodologies. In the figure, "O + SC" refers to the approach that employs the approximate Owen one-sided tolerance limit and the staircase method, and "LRCI" refers to the approach based on the LRCB. The experimental data have been normalized for confidential reasons. For all investigated datasets, the experimental data have been collected with a staircase approach (with at least 15 data) and at least four data for each investigated stress level (at least three or four stress levels).

According to Figure 10, the three approaches provide similar results, with the same trend in the finite fatigue life region and slight differences as concerns the fatigue limit. In general, the LRCB is the most conservative approach, being the estimated fatigue limit below the fatigue limit estimated with the other methods, whereas the bootstrap approach is the least conservative. Accordingly, these three methods can be interchangeably used, if the data are collected with a staircase approach and with tests in the finite life range at three or four stress levels and with at least four data for each stress level. The influence of the number of runout data has been also investigated in the paper, because runout data are the most time-consuming data. It was shown that runout data are fundamental for discriminating if the model shows an asymptotic trend, that is, it ends with a fatigue limit, and also that the number of runout data can be reduced if approaches based on the LRCB and the bootstrap

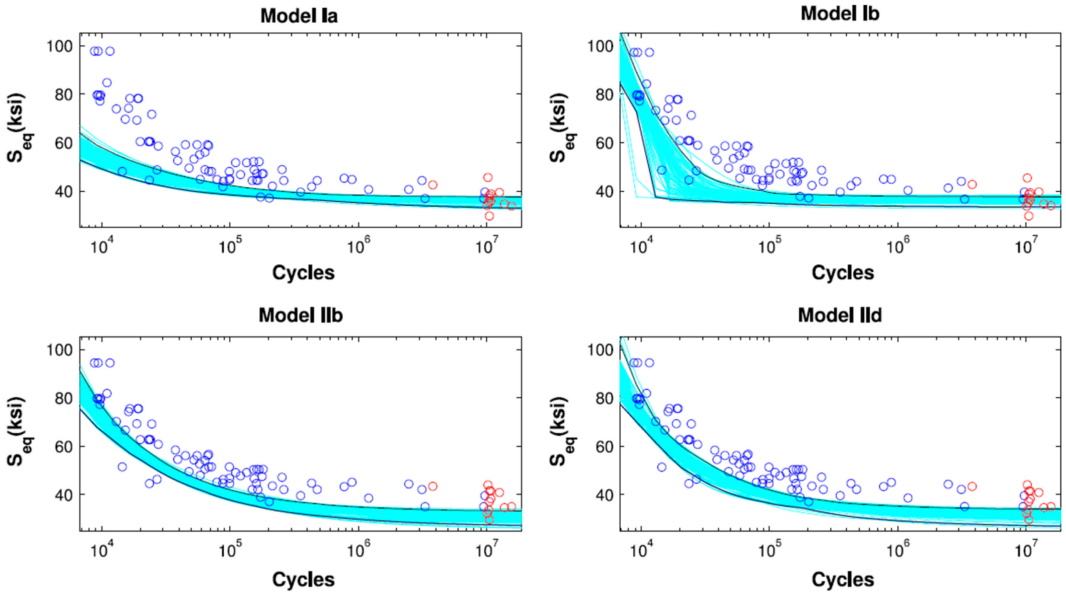

FIGURE 9 | Estimated 95% bootstrap confidence bounds for the 0.05 quantile of the fatigue life with the models investigated in [17]. Reprinted with permission from Elsevier. [Colour figure can be viewed at wileyonlinelibrary.com]

method are employed, avoiding a testing plan based on the staircase approach and optimizing the testing strategy.

4.2 | Stress-Controlled Fatigue Tests: Failures From Defects and VHCF Life Ranges

In this section, the models for the fatigue design P-*S*–*N* curves with failures originating from defects and covering the VHCF life range or the HCF–VHCF life range are analyzed. Actually, even if many statistical models have been proposed for the P-*S*–*N* curves in the VHCF life region [46], a limited number of papers have been dedicated to the design P-*S*–*N* curves in VHCF. However, the fatigue life of components has significantly increased in the last years in many industrial sectors [38, 47–49], and ensuring appropriate safety margins for the design curve even in the VHCF life region is of utmost importance.

The models for design curves of datasets with failures originating from defects and including the VHCF life range have been grouped in this section because failures in VHCF generally originate from defects. However, these models can be employed for failures from defects even in the HCF life region. Indeed, the defect size significantly affects the fatigue response and its influence should be accounted for when the components are to be designed. Section 4.2.1 focuses on design curves estimated by considering datasets with failures originating from defects, whereas Section 4.2.2 is about design curves covering the HCF–VHCF life range and showing a so-called duplex trend.

4.2.1 | Failure Originating From Defects: P-*S*–*N* Design Curves

In this section, models combining the "safe–life" with the "damage-tolerant" approach are analyzed. In [50], datasets involving failures from defects have been investigated, and the design curves have been estimated as LRCB of a specific high-reliability quantile and with the bootstrap approach. In order to model the influence of defects, two types of P-*S*–*N* curves have been introduced: the "conditional P-*S*–*N* curves" and the "marginal P-*S*–*N* curves." The conditional P-*S*–*N* curves are the P-*S*–*N* curve obtained for a specific defect size, that is, conditioned to the defect size, whereas the "marginal P-*S*–*N* curves" are the conditional P-*S*–*N* curve marginalized with the statistical distribution of the defect size. The characteristic defect size is assumed as the square root of the area of the defect projected in a plane perpendicular to the direction of the maximum applied stress [51] and is considered a random variable, $\sqrt{A_c}$, assumed to follow a largest extreme value distribution (LEVD). The cdf of the conditional fatigue life, $F_{Y|\sqrt{a_{d,0}}}(y;x,\sqrt{a_c})$, for a simple linear decreasing trend is given by Equation (23):

$$F_{Y|\sqrt{a_{d,0}}}(y;x,\sqrt{a_c}) = \Phi\left(\frac{y-\mu_Y(x,\sqrt{a_c})}{\sigma_Y}\right) = \Phi\left(\frac{y-(c_Y+m_Y\cdot\log_{10}(s_a)+n_Y\cdot\log_{10}(\sqrt{a_c}))}{\sigma_Y}\right), \quad (23)$$

being c_Y, m_Y, and n_Y constant parameters to be estimated from the experimental data and σ_Y the standard deviation. Accordingly, the term $n_Y\cdot\log_{10}(\sqrt{a_c})$ has been added in the mean of the conditional cdf, assumed to be normally distributed, to account for the influence of the defect size. Starting from Equation (23), the cdf of the marginal fatigue life, $F_Y(y;x)$, is given by

$$F_Y(y;x) = \int_0^\infty F_{Y|\sqrt{a_c}}(y;x,\sqrt{a_c}) f_{\sqrt{A_c}}(\sqrt{a_c})\cdot d\sqrt{a_c}, \quad (24)$$

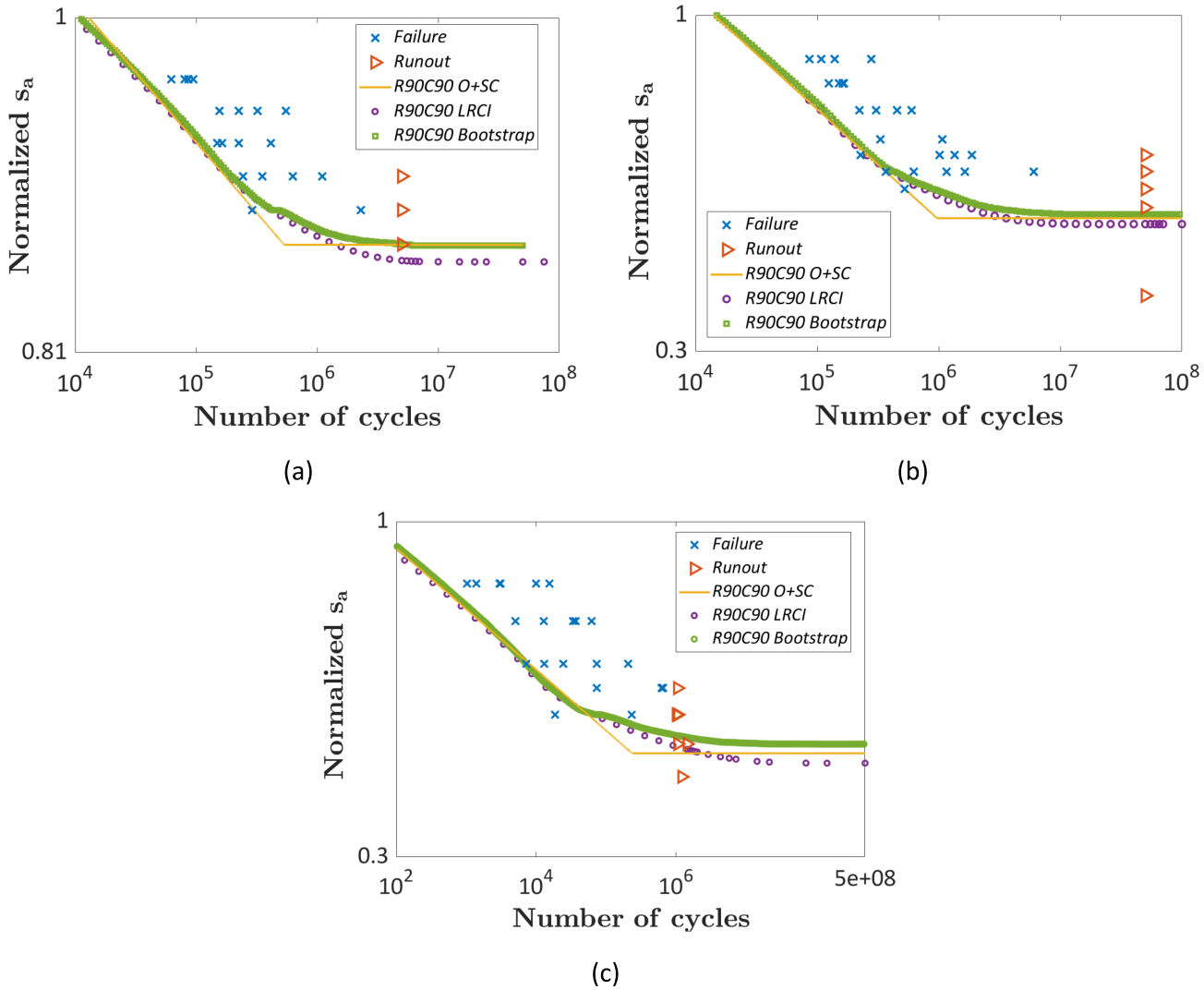

FIGURE 10 | Estimated R90C90 design curves in [8]: (a) TRIP-assisted bainitic steel TBC600Y980T, (b) Aluminum alloy G-AS7C3,5GM, and (c) composite material Polynt SMC LP 2512 R33. Reprinted with permission from Elsevier. [Colour figure can be viewed at wileyonlinelibrary.com]

being $f_{\sqrt{A_c}}(\sqrt{a_c})$ the pdf of the LEVD associated with the defect size. According to [50], more complex experimental trends can be modeled by properly modifying Equations (23) and (24). For example, the cdf of the conditional fatigue life can be modified according to Equation (22) to model an asymptotic trend at the end of the curve. In this case, the cdf of the conditional fatigue life is the product of Equation (23) and the cdf of the fatigue limit, with the mean expressed as a function of the defect size:

being σ_{X_l} the standard deviation and $\mu_{X_l}\left(x, \sqrt{a_{d,0}}\right)$ the mean value of the fatigue limit, with the following expression:

$$F_{Y|\sqrt{a_c}}(y; x, \sqrt{a_c}) = \Phi\left(\frac{y - \mu_Y(x, \sqrt{a_c})}{\sigma_Y}\right) \cdot \Phi\left(\frac{x - \mu_{X_l}(x, \sqrt{a_c})}{\sigma_{X_l}}\right), \tag{25}$$

$$\mu_{X_l}(\sqrt{a_c}) = \frac{c_{sl} \cdot c_{th} \cdot (HV + 120)}{(\sqrt{a_c})^{0.5-\alpha_{th}}}, \tag{26}$$

being HV the material Vickers hardness and c_{sl}, c_{th}, and α_{th} constant material coefficients. According to [50], c_{sl}, c_{th}, and α_{th} can model the formation of a crack directly from a defect or from a defect surrounded by a fine granular area (FGA), the peculiar feature of VHCF failures [52]. The marginal P-S–N curve including a fatigue limit can be obtained by replacing Equation (25) in Equation (24). The procedure for parameter estimation and the estimation of the lower bound of the P-S–N curve with the LRCB is detailed in [50].

For the estimation of the design curve with the bootstrap approach, the procedure is basically the same described in Section 4.1 and in [8], but in this case, a random defect is also estimated starting from the experimental LEVD. Accordingly, for each experimental stress amplitude, a random n_f is estimated starting from a random defect, a random failure probability, and the conditional P-S–N curve. As an example, Figure 11 shows the conditional P-S–N curves (Figure 11a) and the marginal P-S–N curves (Figure 11b) for AlSi10Mg alloy specimens produced through an additive manufacturing (AM) process and tested by the authors. In Figure 11, the 0.1th quantile curve (R90 curve) and the R90C90 design curves estimated with the LRCB ("R90C90 LRCB" curve)

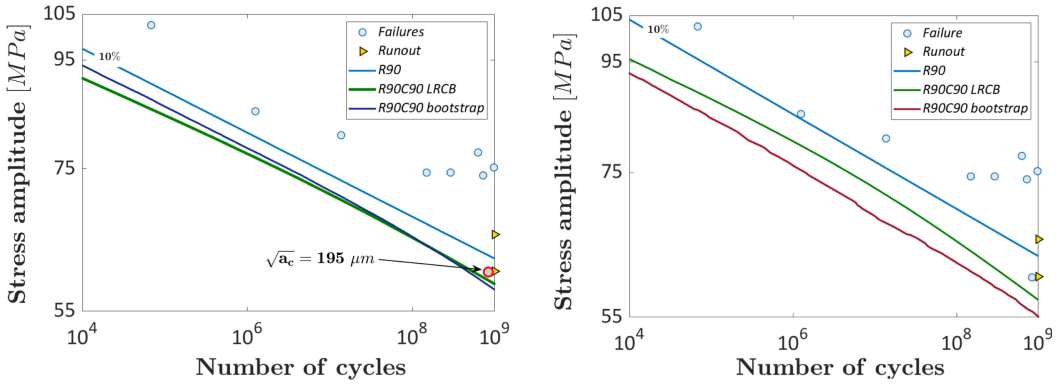

FIGURE 11 | Design curves, estimated with LRCB and bootstrap approaches, for datasets with failures originating from defects: (a) conditional P-*S*–*N* curves and (b) marginal P-*S*–*N* curves [50]. Reprinted with permission from Elsevier. [Colour figure can be viewed at wileyonlinelibrary.com]

and with the bootstrap approach ("R90C90 bootstrap") are shown. For the conditional design curves, a defect with size $\sqrt{a_c} = 195\ \mu$m, that is, the largest defect found experimentally, has been considered.

According to Figure 11, the design curves estimated with the LRCB and bootstrap approaches are in agreement with the experimental data, being below all experimental failures. In particular, they are below the failure originating from the largest defect, differently from the R90 P-*S*–*N* curve. For the conditional design curve, the difference between the LRCB and the bootstrap design curves is limited, whereas the bootstrap design curve is more conservative by considering the marginal model. These two models can be therefore reliably employed for the design curves of datasets with failures originating from defects, combining a "damage tolerance" and a "safe–life" approach.

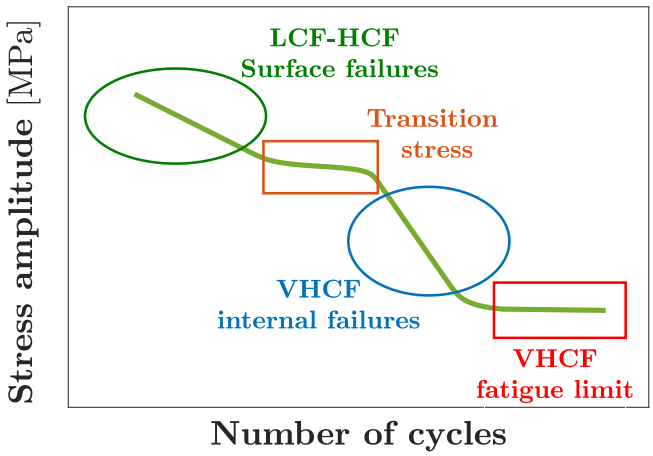

FIGURE 12 | Typical duplex trend for P-*S*–*N* curves covering the HCF–VHCF life range [53]. [Colour figure can be viewed at wileyonlinelibrary.com]

4.2.2 | Duplex P-*S*–*N* Design Curves

In this section, the literature models for datasets showing the so-called duplex trend are reported. The duplex trend, schematically reported in Figure 12, is characterized by a first linearly decreasing trend in the HCF life region, with failures generally originating from the specimen surface, an almost horizontal trend, the so-called "transition stress," a second linearly decreasing trend, with failures originating from internal defects, and a final asymptote, corresponding to the VHCF limit. The transition stress discriminates between surface failures, typical of the HCF life range, and internal failures, typical of VHCF failures.

In [53], the design P-*S*–*N* curves following a duplex trend have been estimated without taking into account the influence of defects in the VHCF life region. The cdf of the fatigue life $F_Y(y;x)$ modeling a duplex trend, according to [54], is reported in Equation (27):

$$F_Y(y;x) = \Phi_{surf}\left(\frac{y-\mu_{Y,surf}(x)}{\sigma_{Y,surf}}\right)\Phi_{Xt}\left(\frac{x-\mu_{X_t}}{\sigma_{X_t}}\right) + \left(1-\Phi_{Xt}\left(\frac{x-\mu_{X_t}}{\sigma_{X_t}}\right)\right)\Phi_{int}\left(\frac{y-\mu_{Y,int}(x)}{\sigma_{Y,int}}\right)\Phi_{Xl}\left(\frac{x-\mu_{X_l}}{\sigma_{X_l}}\right), \quad (27)$$

being Φ_{surf} the cdf of the fatigue life with failures originating from the specimen surface, with mean and standard deviation corresponding to $\mu_{Y,surf}(x)$ and $\sigma_{Y,surf}$, respectively; Φ_{int} the cdf of the fatigue life with failures originating from internal defects, with mean and standard deviation corresponding to $\mu_{Y,int}(x)$ and $\sigma_{Y,int}$, respectively; Φ_{Xt} the cdf of the transition stress, with mean and standard deviation equal to μ_{X_t} and σ_{X_t}, respectively; and Φ_{Xl} the cdf of the VHCF limit, with mean and standard deviation equal to μ_{X_l} and σ_{X_l}, respectively. The mean of the cdf of the fatigue life with failures from surface and internal defects has the form $a \cdot x + b$, to model a linear decreasing trend, with the coefficients a and b being different depending on the failure mode (i.e., surface or internal). In this model, 10 unknown parameters are to be estimated from the experimental data. In [53], the procedure for the estimation of the design curve with the LRCB and by iteratively solving Equation (15), properly rearranged, is provided. Figure 13

shows the design curves for the duplex trend estimated with the approach developed in [53] by considering literature data. Figure 13a shows the R99C90 design curve for a duplex trend without VHCF limit for the SUJ2 steel dataset obtained in [55]. Figure 13b validates the complete duplex trend by considering the dataset reported in [56] and obtained by testing a Ti6Al4V alloy (R90C90 design curve). In Figure 13b, the P-*S*–*N* curves with 10%, 50%, and 90% probability of failure (reliability level of 90%, 50%, and 10%, respectively) are also plotted.

According to Figure 13, the design curves are in agreement with the experimental data and follow the same trend of the experimental failures. Moreover, they are below the experimental failures, ensuring a safety margin with respect to failures, as expected.

Finally, in [50], the design curves for datasets showing a duplex trend and with failures originating from defects in the VHCF life range have been estimated. The initial model is the same reported in Equation (27) but modified with Equations (24)–(26) to take into account the influence of defects. The design curves have been estimated as LRCB, by solving Equation (15), and with a bootstrap approach, by considering also the LEVD followed by the defect size, as detailed in [50]. Figure 14 shows the design curves estimated for a dataset obtained through tests on an H13 steel in [57, 58]. The 0.1th quantile P-*S*–*N* curve ("R90") and the R90C90 design curves estimated with the bootstrap ("R90C90 bootstrap") approach and as LRCB ("R90C90 LRCB") are shown.

According to Figure 14, the two models agree with the experimental data, being capable of following the duplex trend. However, the R90C90 LRCB is closer to the experimental data and more properly adapts to the experimental failures, whereas the R90C90 bootstrap design curve is more conservative in the VHCF life region and, for the investigated life range, cannot model the asymptotic trend of the VHCF limit. The R90C90 LRCB design curve is therefore to be preferred due to the complexity in the simulation and replication of the original dataset with the bootstrap approach.

5 | Discussion

In this section, the analyses carried out in previous sections are recalled and further extended, to try to highlight the strengths and the weaknesses of the investigated approaches and provide general considerations that can be useful for guiding the choice of the appropriate approach when components are to be designed. Table 2 summarizes the industrial approaches and, if available, the required reliability levels for specific applications, according to the literature analyses. In particular, for each method, the main application field, if it has been applied for strain/stress–life data and the associated references are reported.

According to Table 2, the general trend in industrial applications is towards simple procedures for the assessment of the design curves or the design points. This can be justified by considering that fatigue experimental tests are time consuming and the following analysis of the experimental data is expected to be straightforward, ensuring however the required reliability. This explains why methodologies based on shifting the median curve or the best-fitting experimental stress/strain–life curve by a safety margin obtained by multiplying the standard deviation by an appropriate safety factor are among the most used methodologies. A factor corresponding to two or three times the standard deviation or a factor of 20 (by considering the number of cycles to failure) or 2 (by considering the strain or the stress amplitude) are largely employed, depending on the application. However, this approach is based on empirical safety factors which try to model the experimental uncertainty or the influence of specific factors (e.g., size effect or the influence of water coolant in nuclear applications) but do not take into account the actual statistical distribution of the fatigue life or the uncertainty associated with the parameter estimation. The "approximate Owen one-side tolerance limit" and similar approaches allow to overcome these weaknesses, with the safety factor depending on sample size, reliability, and confidence targets, available in literature tables. The analyses carried out in [14] have moreover proven that shifting the median curve by a fixed factor corresponding to two or three times the standard deviation provides less conservative design curves. The result in [14] cannot be generalized, since

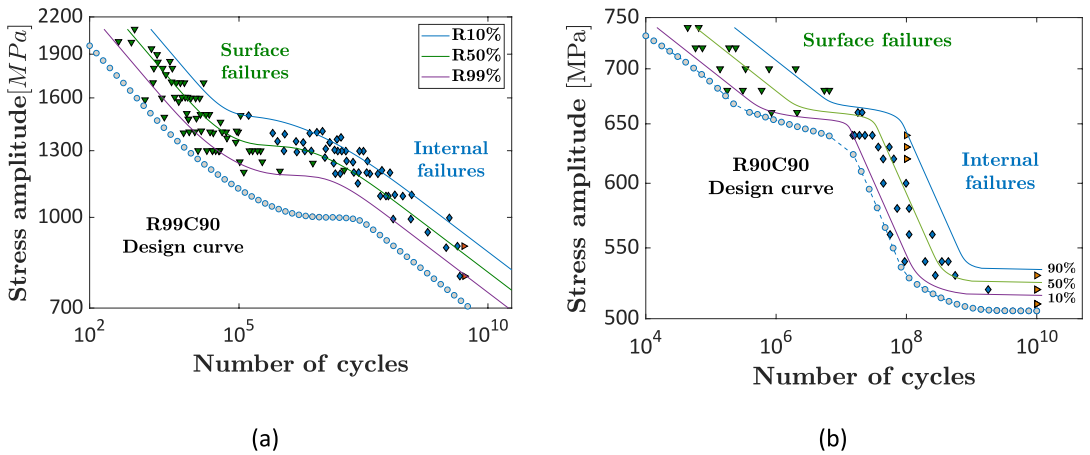

FIGURE 13 | Validation of the model in [53] for the design curves of datasets showing a duplex trend in the range HCF–VHCF: (a) model without the VHCF limit with the dataset available in [55] and (b) complete model for the dataset reported in [56] and obtained by testing a Ti6Al4V alloy. [Colour figure can be viewed at wileyonlinelibrary.com]

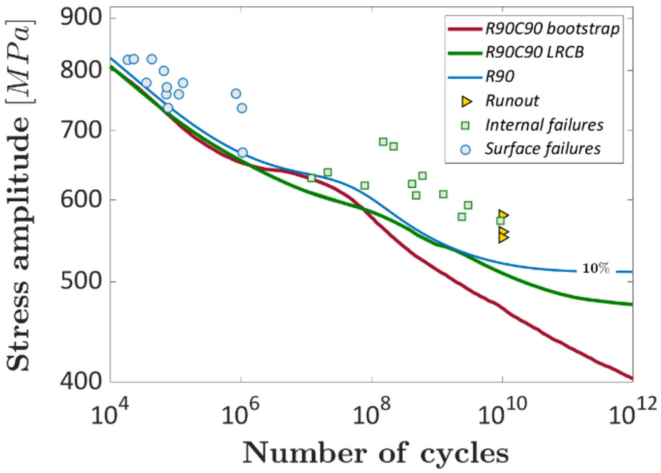

FIGURE 14 | Duplex P-*S*–*N* curves with failures originating from defects in the VHCF life range: R90C90 design curves estimated with the bootstrap approach and with the LRCB [50]. Reprinted with permission from Elsevier. [Colour figure can be viewed at wileyonlinelibrary.com]

dependent on the dataset and its variability, but confirms that the sample numerosity, reliability, and confidence targets should be carefully considered for a safe design of components. The results obtained with approaches based on shifting the median curve can be moreover easily implemented in FE codes, which generally require the slope and the intercept of the estimated design curve or the fatigue limit. For example, for datasets showing a linearly decreasing trend and a fatigue limit, the slope and the intercept of the linear trend are required, together with the fatigue limit value. These parameters can be easily extracted with the methodologies based on shifting the best-fitting curve (or the lower bound fatigue limit estimated with the staircase).

On the other hand, the models developed in the academic literature are more complex and require in many cases an implementation with numerical software to assess the design curve. Beretta et al. [18, 19] have interestingly developed a format for failure probability for components subjected to LCF loads, focusing on the importance of modeling and also the variability associated with the loads when the design point at the required reliability target is to be assessed. The method in [19] for multiaxial loads requires the integration of FE simulations and numerical software to assess the design point. The assessment of the design curves by exploiting the profile likelihood properties and the LRCB has gained significant interest in the last years. The design curves in [8, 15, 35, 50, 53] have been obtained as the LRCB of a high-reliability quantile P-*S*–*N* curve. This approach ensures a better coverage probability, it does not require an assumption on the shape or the distribution of the confidence intervals and, according to [61], methodologies based on the LRCB "perform well even in small samples." On the other hand, these methods require a complex implementation and an iterative procedure based on repeated optimizations. However, it must be noted that these methodologies can be automated, and therefore, after the first time-consuming implementation stage, the results can be obtained in a quite limited amount of time. Another drawback is that the LRCB design curves cannot be passed directly as material input in FE code, because they are not described by an analytical expression but obtained point by point. However, the obtained design curve can be linearized through appropriate strategies, as discussed in [8]. Similar considerations can be made for design curves based on the bootstrap approach, which requires a rather simple implementation but the estimation phase can be more time consuming, because a large number of datasets should be randomly generated. Moreover, the bootstrap approach is strongly dependent on the initial estimation of the unknown parameters, and this must be carefully taken into account when employed. The Bayesian approach [45] for the assessment of the design curve represents a valid alternative to the above-described methodologies, based on classical inference theory. It can be useful when the available experimental dataset is limited, but it relies on prior knowledge on the material parameters, which are generally not available with a high degree of reliability.

The statistical distribution of the fatigue life should be also discussed. In almost all investigated models, a log-normal distribution has been employed for the fatigue life, regardless of the type of considered load (strain or stress). This confirms that the log-normal distribution can be reliably employed for modeling the fatigue life. In [15], the fatigue life and the fatigue limit have been also assumed to follow a SEV distribution, providing more conservative results. In the literature, other statistical distributions have been also used for the fatigue life. For example, in [9, 62], the authors have shown that only the Weibull distribution should be used for the lower bound of the design curve. The models proposed in the literature, however, are flexible and could be also quite easily extended to other statistical distributions for the fatigue life that may better fit the experimental data and could work better for lower bound design curves.

The methodology employed for parameter estimation is also very important. The design methodologies used in the literature and based on shifting the best-fitting curve are based on the estimation of the linearly decreasing trend with the least square method. This approach, however, does not allow to consider runout data, which, on the contrary, contain important information that cannot be neglected. The MLP, on the other hand, permits to consider both failure and runout data, allowing for a more effective estimation and avoiding losing the information contained in the runout data, which are, on the other hand, the most time-consuming data. For example, International Standard ASTM E739 recommends the use of the MLP, or in [63], it was shown that methodologies based on the MLP allow for more efficient estimations of the fatigue response. MLP is particularly effective when combined with statistical models describing both the finite life range and the fatigue limit, as the "random fatigue limit model" or the models proposed in [8]. With these models, the parameter estimation is carried out simultaneously and not separately, as in the procedure reported in [10], which requires a staircase and tests at different levels to estimate the linear trend and the fatigue limit. By employing the "continuous" statistical models in [8, 15, 16], the test strategy can be optimized, with a possible reduction of the number of runout data and significantly enhancing the test efficiency, as demonstrated in [8]. With these approaches, moreover, no assumptions are to be made on the trend of the experimental data, because the

TABLE 2 | Summary of the industrial practice for the assessment of the design curves and the design points in specific applications.

Method	Main applications	Strain/stress–life	Standard or reference
Median curve shifted by two or three times the standard deviation	Industrial applications in general	Both strain/stress–life model	[10]
Approximate Owen one-side tolerance limit	Industrial applications in general	Both strain/stress–life model	[10, 13, 21]
Shift of the best-fit curve by a factor of 20 by considering the number of cycles to failure	Nuclear applications	Strain–life model	[30]
Shift of the best-fit curve by a factor of 2 by considering the strain amplitude	Nuclear applications	Strain–life model	[30]
Median fatigue strength shifted by one-side lower bound tolerance limit K factor for a normal distribution	Industrial applications in general	Staircase approach	[10, 22]
Failure probability of 5% and a safety factor $\gamma_F = 1.35$ for S–N diagram	Welding applications details	S–N diagram	[12, 18]
Failure probability of 5% and a safety factor $\gamma_F = 1.5$ for S–N diagram	Steel and aluminum components	S–N diagram	[18, 59]
Failure probability of 10^{-3}	Aeroengine components	Stress–life curve	[19]
$\frac{TOS}{\mu - 3 \cdot \sigma}$ methodology:mean fatigue strength shifted by three standard deviations and "extreme load spectrum" defined as three standard deviations above the mean	Helicopter components	Stress–life model	[19, 60]

parameters ensuring the best fitting of the data are provided in output from the ML. For example, if an asymptotic trend is not present or not suggested by the available data, the best-fitting curve will be characterized by only a linear decreasing trend, even if the initial statistical model has a fatigue limit. On the other hand, with the approach in [10], combining the staircase and the approximate one-side tolerance limit, a fatigue limit is imposed and it will correspond to the lower bound stress estimated with the staircase approach, even if not suggested by the experimental data.

A last point of discussion, which has emerged from the analyses carried out in this paper, regards the VHCF life range. Indeed, the literature on the design curves in the VHCF life range is scarce, even if the fatigue life of components has significantly increased in the last years and possible failures in this life regime, especially from internal defects [50, 53], are to be considered during the design stage.

To conclude, future research should focus on the definition of optimized design curves that can ensure a reliable safety margin with respect to failures, without being too conservative, to avoid an overdesign and a consequent possible weight increment. Future research should also focus on defining statistical models capable of better fitting the experimental data and allowing to define more efficient experimental strategies for a reliable estimation of the design curves, possibly combined with machine learning algorithms that may facilitate the parameter estimation with automated procedures and the implementation in FE codes.

6 | Conclusions

In the paper, a review on the methodologies currently available for the assessment of the fatigue probabilistic-stress/strain design curves is provided. The design curves should ensure a reliable safety margin with respect to failures and are used for a safe fatigue design of components. Methodologies for the design curves currently employed in industrial applications and research papers have been reviewed.

The following general conclusions can be drawn:

1. The methods involving a shift of the median curve or the best-fitting curve by a safety margin obtained by multiplying the standard deviation by a conservative factor are the most used in industrial applications.
2. A fixed conservative factor, generally corresponding to two or three times the standard deviation, is less effective than factors dependent on the dataset numerosity, the required reliability and confidence targets.
3. The least square method is generally employed for the parameter estimation. However, methodologies like the Maximum Likelihood Principle, allowing to consider both failure and runout data, are recommended.
4. Methodologies based on the likelihood ratio confidence lower bound or the bootstrap approach have proven effective in estimating the design stress/strain–life curves, even if they required a more complex and not straightforward implementation and the use of numerical software.

5. Methodologies for the design curves have focused mainly on the Low Cycle Fatigue and the High Cycle Fatigue life ranges. However, the research should focus also on the design curves for the Very High Cycle Fatigue life range, because the expected fatigue life of components is significantly longer than in the past.

Author Contributions

Andrea Tridello: formal analysis, writing – original draft, visualization. **Carlo Boursier Niutta:** formal analysis, writing – review and editing. **Massimo Rossetto:** writing – review and editing. **Filippo Berto:** writing – review and editing. **Davide S. Paolino:** writing – review and editing.

Acknowledgments

Open access publishing facilitated by Politecnico di Torino, as part of the Wiley - CRUI-CARE agreement.

Data Availability Statement

Data sharing is not applicable to this article as no new data were created or analyzed in this study.

References

1. S. K. Bhaumik, M. Sujata, and M. A. Venkataswamy, "Fatigue Failure of Aircraft Components," *Engineering Failure Analysis* 15 (2008): 675–694.

2. U. Zerbst, M. Madia, C. Klinger, D. Bettge, and Y. Murakami, "Defects as a Root Cause of Fatigue Failure of Metallic Components. I: Basic Aspects," *Engineering Failure Analysis* 97 (2019): 777–792.

3. R. I. Stephens, A. Fatemi, R. R. Stephens, and H. Fuchs, *Metal Fatigue in Engineering*, 2nd ed. (Hoboken, NJ: Wiley, 2000).

4. ASTM E739-10, "Standard Practice for Statistical Analysis of Linear or Linearized Stress-Life (S-N) and Strain-Life (ε-N) Fatigue Data," (2015).

5. BS ISO12107:2003, "Metallic Materials—Fatigue Testing—Statistical Planning and Analysis of Data," 3rd ed. (2003).

6. ASTM E606/E606M-21, "Standard Test Method for Strain-Controlled Fatigue Testing," (2021).

7. H. Usabiaga, M. Muniz-calvente, M. Ramalle, I. Urresti, and A. F. Canteli, "Improving With Probabilistic and Scale Features the Basquin Linear and Bi-Linear Fatigue Models," *Engineering Failure Analysis* 116 (2020): 104728.

8. A. Tridello, C. Boursier Niutta, F. Berto, et al., "Design Against Fatigue Failures: Lower Bound P-S-N Curves Estimation and Influence of Runout Data," *International Journal of Fatigue* 162 (2022): 106934.

9. E. Castillo and A. Fernandez-Canteli, *A Unified Statistical Methodology for Modeling Fatigue Damage* (New York City: Springer, 2009).

10. Y. Li Lee, J. Pan, R. Hathaway, and M. Barkey, *Fatigue Testing and Analysis: Theory and Practice* (New York: Elsevier B.V., 2005).

11. CEN European Committee for Standardization, "Eurocode 9—Design of Aluminium Structures—Part 1–3: Structures Susceptible to Fatigue," (2021).

12. (2005) EN 1993-1-9, "Eurocode 3: Design of Steel Structures—Part 1–9: Fatigue," (2005).

13. C. R. Williams, Y. L. Lee, and J. T. Rilly, "A Practical Method for Statistical Analysis of Strain-Life Fatigue Data," *International Journal of Fatigue* 25 (2003): 427–436.

14. D. Benasciutti, J. Srnec Novak, L. Moro, and F. De Bona, "Experimental Characterisation of a CuAg Alloy for Thermo-Mechanical Applications. Part 2: Design Strain-Life Curves Estimated via Statistical Analysis," *Fatigue and Fracture of Engineering Materials and Structures* 41 (2018): 1378–1388.

15. F. G. Pascual and W. Q. Meeker, "Estimating Fatigue Curves With the Random Fatigue-Limit Model," *Technometrics* 41 (1999): 277–290.

16. S. Loren, "Fatigue Limit Estimated Using Finite Lives," *Fatigue and Fracture of Engineering Materials and Structures* 26 (2003): 757–766.

17. I. Babuška, Z. Sawlan, M. Scavino, B. Szabó, and R. Tempone, "Bayesian Inference and Model Comparison for Metallic Fatigue Data," *Computer Methods in Applied Mechanics and Engineering* 304 (2016): 171–196.

18. S. Beretta, S. Foletti, E. Rusconi, A. Riva, and D. Socie, "A Log-Normal Format for Failure Probability Under LCF: Concept, Validation and Definition of Design Curve," *International Journal of Fatigue* 82 (2016): 2–11.

19. S. P. Zhu, S. Foletti, and S. Beretta, "Probabilistic Framework for Multiaxial LCF Assessment Under Material Variability," *International Journal of Fatigue* 103 (2017): 371–385.

20. D. Owen, "A Survey of Properties and Applications of the Noncentral t-Distribution," *Technometrics* 10 (1968): 445–472.

21. C. L. Shen, P. H. Wirshing, and G. T. Cashman, "Design Curve to Characterize Fatigue Strength," *Journal of Engineering Materials and Technology* 118 (1996): 535–541.

22. C. L. Shen, *The Statistical Analysis of Fatigue Data*" (PhD Thesis (Tucson, AZ, USA: Arizona University, 1994).

23. S. S. Manson, "Behavior of Materials Under Conditions of Thermal Stress," (1953).

24. L. Coffin and N. Y. Schenectady, "A Study of the Effects of Cyclic Thermal Stresses on a Ductile Metal," *Transaction ASME* 76 (1954): 931–949.

25. J. Morrow, "Fatigue Properties of Metals," in *Fatigue Design Handbook Experimental Mechanics* (Warrendale, PA: Society of Automotive Engineers, 1964).

26. A. Fatemi, A. Plaseied, A. K. Khosrovaneh, and D. Tanner, "Application of Bi-Linear Log-Log S-N Model to Strain-Controlled Fatigue Data of Aluminum Alloys and Its Effect on Life Predictions," *International Journal of Fatigue* 27 (2005): 1040–1050.

27. J. Morrow, *Cyclic Plastic Strain Energy and Fatigue of Metals* (West Conshohocken, Pennsylvania: ASTM, 1965), 45–86.

28. P. H. Wirsching, "Statistical Summaries of Fatigue Data for Design Purposes. NASA Report 3697," (1983).

29. P. H. Wirsching and S. Hsieh, "Linear Model in Probabilistic Fatigue Design," *Journal of the Engineering Mechanics Division* 106 (1980): 1265–1278.

30. "ASME Boiler & Pressure Vessel Design Code—III Div. 1—Rules for Construction of Nuclear Facility Components," (2005).

31. Argonne National Library Final Report, "Effect of LWR Coolant Environments on the Fatigue Life of Reactor Materials," (2007).

32. J. M. Keisler, O. K. Chopra, and W. J. Shack, "Statistical Models for Estimating Fatigue Strain-Life Behavior of Pressure Boundary Materials in Light Water Reactor Environments," *Nuclear Engineering and Design* 167 (1996): 129–154.

33. D. Taylor and Y. L. Lee, "Validation of the Statistical Strain-Life Design Curves for Various Grades of Sheet Steel," *SAE Transactions* 113 (2004): 320–327.

34. D. G. Harlow, "Statistical Modeling for Low Cycle Fatigue," in *TMS 2014: 143rd Annual Meeting & Exhibition* (Cham: Springer, 2014), 639–646.

35. A. Tridello and D. S. Paolino, "LCF-HCF Strain–Life Model: Statistical Distribution and Design Curves Based on the Maximum Likelihood Principle," *Fatigue and Fracture of Engineering Materials and Structures* 46 (2023): 2168–2179.

36. B. Pyttel, D. Schwerdt, and C. Berger, "Very High Cycle Fatigue—Is There a Fatigue Limit?," *International Journal of Fatigue* 33 (2011): 49–58.

37. A. Fernández-Canteli, S. Blasón, B. Pyttel, M. Muniz-Calvente, and E. Castillo, "Considerations About the Existence or Non-Existence of the Fatigue Limit: Implications on Practical Design," *International Journal of Fracture* 223 (2020): 189–196.

38. C. Bathias and P. C. Paris, *Gigacycle Fatigue in Mechanical Practice* (Cleveland, OH: CRC Press, 2004).

39. S. Romano, A. Brückner-Foit, A. Brandão, J. Gumpinger, T. Ghidini, and S. Beretta, "Fatigue Properties of AlSi10Mg Obtained by Additive Manufacturing: Defect-Based Modelling and Prediction of Fatigue Strength," *Engineering Fracture Mechanics* 187 (2018): 165–189.

40. Y. X. Zhao, "A Probabilistic Assessment of the Design S-N Curves for 1Cr18Ni9Ti Pipe-Welded Joint," *Journal of Pressure Vessel Technology* 125, no. 2 (2003): 195–200.

41. J. Collins, *Failure of Materials in Mechanical Design—Analysis, Prediction, and Prevention* (Hoboken, NJ: Wiley, 1993).

42. W. J. Dixon, "The Up-and-Down Method for Small Samples," *Journal of the American Statistical Association* 60 (1965): 967–978.

43. W. J. Dixon, "A Method for Obtaining and Analyzing Sensitivity Data," *Journal of the American Statistical Association* 43 (1948): 109–126.

44. G. Lieberman, *Tables for One-Sided Statistical Tolerance Limits. LIE ONR 34* (Stanford, CA: Stanford University, Department of Statistics, 1957).

45. M. Guida and F. Penta, "A Bayesian Analysis of Fatigue Data," *Structural Safety* 32 (2010): 64–76.

46. A. Tridello, C. Boursier Niutta, M. Rossetto, F. Berto, and D. S. Paolino, "Statistical Models for Estimating the Fatigue Life, the Stress–Life Relation, and the P-S–N Curves of Metallic Materials in Very High Cycle Fatigue: A Review," *Fatigue and Fracture of Engineering Materials and Structures* 45 (2022): 332–370.

47. C. Bathias and P. C. Paris, "Gigacycle Fatigue of Metallic Aircraft Components," *International Journal of Fatigue* 32 (2010): 894–897.

48. E. Bayraktar, I. M. Garcias, and C. Bathias, "Failure Mechanisms of Automotive Metallic Alloys in Very High Cycle Fatigue Range," *International Journal of Fatigue* 28 (2006): 1590–1602.

49. A. A. Shanyavskiy, "Very-High-Cycle-Fatigue of In-Service Air-Engine Blades, Compressor and Turbine," *Science China—Physics Mechanics & Astronomy* 57 (2014): 19–29.

50. A. Tridello, C. B. Niutta, M. Rossetto, F. Berto, and D. S. Paolino, "Statistical Estimation of Fatigue Design Curves From Datasets Involving Failures From Defects," *International Journal of Fatigue* 176 (2023): 107882.

51. Y. Murakami, *Metal Fatigue: Effects of Small Defects and Nonmetallic Inclusions* (Amsterdam, The Netherlands: Elsevier, 2002).

52. J. P. Sippel and E. Kerscher, "Properties of the Fine Granular Area and Postulated Models for Its Formation During Very High Cycle Fatigue—A Review," *Applied Sciences* 10, no. 23 (2020): 8475.

53. A. Tridello, C. B. Niutta, F. Berto, M. Rossetto, and D. S. Paolino, "Duplex LCF-VHCF P-S-N Design Curves: A Methodology Based on the Maximum Likelihood Principle," *Procedia Structural Integrity* 42 (2022): 1320–1327.

54. D. S. Paolino, G. Chiandussi, and M. Rossetto, "A Unified Statistical Model for S-N Fatigue Curves: Probabilistic Definition," *Fatigue and Fracture of Engineering Materials and Structures* 36 (2013): 187–201.

55. T. Sakai, B. Lian, M. Takeda, et al., "Statistical Duplex S-N Characteristics of High Carbon Chromium Bearing Steel in Rotating Bending in Very High Cycle Regime," *International Journal of Fatigue* 32 (2010): 497–504.

56. *NIMS Fatigue Data Sheet No. 98. Data Sheet on Giga-Cycle Fatigue Properties of Ti–6Al–4V (1100 MPa Class) Titanium Alloy* (Tokyo: National Institute for Materials Science).

57. R. Yeşildal, "The Effect of Heat Treatments on the Fatigue Strength of H13 Hot Work Tool Steel," Preprint, (2018).

58. A. Tridello, "VHCF Response of Two AISI H13 Steels: Effect of Manufacturing Process and Size-Effect," *Metals (Basel)* 9 (2019): 133.

59. FKM Guideline, *Analytical Strength Assessment of Components in Mechanical Engineering*, 6th ed. (Frankfurt: VDMA Verlag, 2012).

60. Y. Tong, *Literature Review on Aircraft Structural Risk and Reliability Analysis. Tech Rep DSTR-1306* (Melbourne, Australia: DSTO Aeronautical and Maritime Research Laoratory, 2001).

61. G. Ostrouchov and W. Q. Meeker, "Accuracy of Approximate Confidence Bounds Computed From Interval Censored Weibull and Lognormal Data," *Journal of Statistical Computation and Simulation* 29 (1988): 43–76.

62. B. Pyttel, A. F. Canteli, and A. A. Ripoll, "Comparison of Different Statistical Models for Description of Fatigue Including Very High Cycle Fatigue," *International Journal of Fatigue* 93 (2016): 435–442.

63. M. L. Facchinetti, "Fatigue Tests for Automotive Design: Optimization of the Test Protocol and Improvement of the Fatigue Strength Parameters Estimation," *Procedia Engineering* 133 (2015): 21–30.